SynOpen A. Kumar et al. THIEME OPEN ACCESS Review

Recent Advancements in Triazole-based Click Chemistry in Cancer Drug Discovery and Development

Arun Kumar[a]
Ashok Kumar Yadav*[b]
Vivek Mishra*[c]
Deepak Kumar*[a]

[a] Department of Pharmaceutical Chemistry, School of Pharmaceutical Sciences, Shoolini University of Biotechnology and Management Sciences, Solan, Himachal Pradesh, 173229, India
guptadeepak002@gmail.com
[b] University Institute of Pharmaceutical Sciences, Panjab University, Chandigarh, 160014, India
ashoky@pu.ac.in
[c] Amity Institute of Click Chemistry Research and Studies, Amity University, Noida, Uttar Pradesh, 201301, India
vmishra@amity.edu

Published as part of the Virtual Collection
Click Chemistry and Drug Discovery

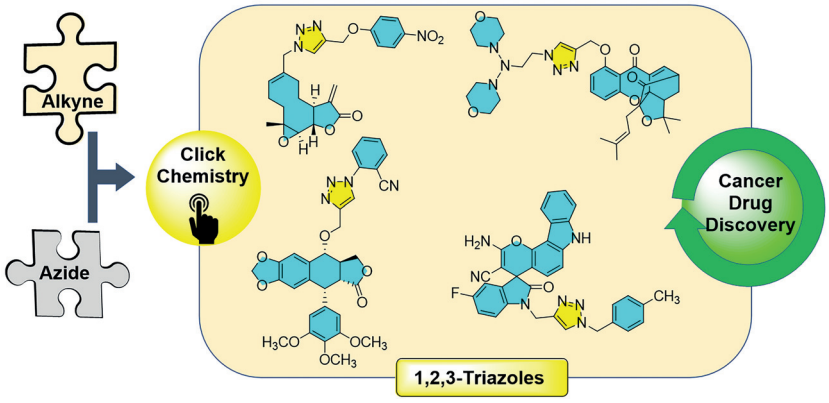

Received: 28.01.2023
Accepted after revision: 30.03.2023
Published online: 17.05.2023 (Version of Record)
DOI: 10.1055/s-0042-1751452; Art ID: SO-2023-01-0010-RV

Abstract Triazole-based compounds possess a broad range of activity and can be synthesized using click chemistry. Many new chemotherapeutic agents have been developed in recent years by exploiting click chemistry and these are covered in this review.

Key words click chemistry, cycloaddition, triazoles, cancer, chemotherapy

1 Introduction

Cancer ranks as one of the top causes of mortality globally and caused around 10 million deaths in 2020 (accounting for one of every six deaths).[1] Chemotherapy has been an important part of cancer therapy alongside surgery and radiotherapy and has helped to reduce cancer cases over time in developed countries like the USA.[2] But on a larger scale there is a constant need to develop newer molecules with less toxicity and more selectivity to tackle resistance and improve the effectiveness of the chemotherapy.[3] However, there are a few drawbacks, for example curcumin has low water solubility, poor absorption, and quick metabolism, which restrict its therapeutic efficacy.[4] According to reports, the separate administration of a chemotherapeutic agent is still difficult due to clinical limits such as high toxicity, the development of multidrug resistance, and other side effects.[5,6] Due to the various pharmacokinetics and metabolic actions of these medications, it is typically difficult to mix two or more free agents into a 'cocktail' formulation to obtain optimal antitumor activity.[7,8] Actually, effective distribution of two or more chemotherapeutic drugs through combination therapy has been shown to be a sophisticated and effective method for treating a variety of malignancies.[9–12] To the best of our knowledge, the current dual-drug delivery system has always used the strategies of physical embedding, noncovalently binding by hydrophobic interactions, or electrostatic adherence, which would have some drawbacks, including the premature release of the drug due to the unstable structure and difficulty controlling and modifying the drug release rate.[13]

2 Triazole Properties as Pharmacophore

There are many methods for the synthesis of triazole rings but click chemistry is a rapid, selective, and reliable method for triazole synthesis.[14,15] Since its introduction by Meldal and Sharpless[14,16] click chemistry has been used in polymers,[17,18] materials science,[19–24] drug discovery,[25–27] bioconjugation,[28–32] and organic chemistry.[33–38] The most common reaction in click chemistry is the copper(I)-catalyzed 1,3-dipolar cycloaddition of alkynes and azides to form 1,2,3-triazoles.[39,40] Triazole, a heterocycle[41–43] is found in many natural and synthetic compounds and has a wide spectrum of use in materials science, protective materials,[44] and agriculture.[45] Triazoles are also known to be of great pharmaceutical importance as their derivatives are found to have anticancer,[46] antiproliferative,[47] antiviral,[48] antimalarial,[49] antineoplastic,[50] anticonvulsant,[51] local anesthetic, anti-inflammatory,[52] analgesic,[53] and antimicrobial activities.[54–58]

Biographical Sketches

Arun Kumar received his Master of Pharmacy in Pharmaceutical Chemistry from Shoolini University in 2020 and is currently following his Ph.D. in Pharmaceutical Sciences at Shoolini University. His research interests include the synthesis of medicinally important compounds and computational studies.

Dr. Ashok Kumar Yadav was born in U. P., India. He obtained his M.Sc. (Chemistry, 1999) from the University of Lucknow, India. In 2002, he started his Ph.D. in Chemistry at the Department of Chemistry, Indian Institute of Technology, Kanpur, India, and his Ph.D. degree was awarded in 2008 from UP Technical University, India. From June 2010 to June 2012, he worked as a postdoctoral researcher at the University of Antwerp, Belgium and from August 2012 until July 2013 he was a postdoctoral research fellow at the Universität Leipzig, Germany. He worked as DST Fast Track Young Scientist at Centre of Biomedical Research (CBMR), India from 2014 to 2017. He is currently a UGC Assistant Professor at the University Institute of Pharmaceutical Sciences, Panjab University, Chandigarh, India (since 2018). His research interests lie in the development of new synthetic methodology, API synthesis and process development, development of new biologically active molecules against diabetes and bacterial infection and further to find out their applications for the development of drugs.

Dr. Vivek Mishra is currently working as Assistant Professor-III in Amity Institute of Click Chemistry Research and Studies, Amity University, Noida, Uttar Pradesh, India. He received his Ph.D. from the Department of Chemistry, Banaras Hindu University, Varanasi. He carried out his postdoctoral studies at the Green Process and Material R&D Laboratory, Korea Institute of Industrial Technology, South Korea and at Functional Material Research Laboratory, University of Ulsan, South Korea. He is also a recipient of SERB-Teachers Associateship for research Excellence (TARE) Fellow (October 2022) and SERB-National Postdoctoral Fellow in Green Chemistry Network Centre, University of Delhi. His research work mainly focuses on organic chemistry, green chemistry, click chemistry, polymer chemistry, advanced functional material, and forensic sciences. Currently, he has several publications in leading chemistry, forensic, and polymer journals and holds 4 international patents (granted) and 3 Indian Patent (filed in 2022). He is Guest editor of various international journals and has also published several international books and book chapters in Elsevier, CRC Press, Wiley-Scrivener, etc.

Dr. Deepak Kumar has worked as a Professor at the Department of Pharmaceutical Chemistry, School of Pharmaceutical Sciences, Shoolini University, India since 2017. Dr. Kumar received his Ph.D. from CWNU, South Korea under the prestigious Brain Korea 21Plus fellowship. He also worked as National Research Foundation Fellow South Korea; Teaching and Research Assistant in CNU, S. Korea. Prior to that, he received his M.Pharm. from Sikkim Central University, Sikkim, and B.Pharm. from Uttar Pradesh Technical University, Lucknow. His research areas include medicinal chemistry and drug discovery; bioorganic chemistry; drug delivery; nanomedicine; and chemical biology; design and synthesis diversified bioactive small molecules and their application in chemical biology and medicinal chemistry; total synthesis of natural products for biological activities; diversity-oriented synthesis of novel heterocycles; target-based approaches to access novel small molecules as drugs for type II diabetes and cancer.

The significance of the 1,2,3-triazole scaffold in the field of medicinal chemistry has increased because of some special properties, such as tendency to form hydrogen bonds, dipole-dipole and stacking interactions of triazole compounds, as well as their familiarity to amide bonds regarding distance and planarity.[59,60] These properties strongly favor to bind with the biomolecular targets. This well-known heterocyclic pharmacophore has the added benefits of improving cell permeability and target binding and is quite resistant to biotransformation.[61] It is also capable of contributing to dipole-dipole interactions and hydrogen bonding. Synthetic methods based on the click strategy offer effective routes for the quick and gentle production of bioactive leads as potential candidates for enzyme inhibitory activities. Moreover, the triazole motif has the additional benefits of being a suitable linker group because of its outstanding planar stability against metabolism biotransformation, the aromatic nature of the triazole core, as well as the defined dipole moment and H-bonding formation.[62,63] On the other hand, it has been discovered that combining many pharmacophores into a single hybrid structure is an effective method for creating novel molecules with exciting activities.[64] In the presence of a copper catalyst, the 1,2,3-triazole ring might be joined to a carboxylic group to create a water-soluble ester.[14] Usually, the best option for increasing the cell permeability of COOH-bearing molecules is esterification. Unfortunately, such a straightforward esterification invariably results in a severe loss of water solubility and lowers bioavailability for oral administration or injection. Click chemistry has been exploited largely to synthesize triazole-based molecules and delivery systems, some recent uses of click chemistry of such importance are discussed in this review.

3 Click Chemistry in Compound Synthesis

Noodleman, Sharpless, Fokin, and co-workers predicted two competitive pathways for Cu(I)-catalyzed azide-alkyne cycloaddition (CuAAC) using DFT calculations in 2005, a slow process catalyzed by a mononuclear Cu species (Pathway A) and a more kinetically favored route promoted by the formation of a dinuclear Cu catalyst (Pathway B). There is usually a tremendous conflict to confirm by which pathway the click reaction is taking place (Figure 1).[65] By following these mechanisms, various researchers have developed and explained the importance of triazoles in oncology drugs which are synthesized via click chemistry.

Triazole-based naphthalene-1,4-dione compounds tested for their anticancer activity on MOLT-4, MCF-7, and HT-29 cells were synthesized via copper-catalyzed click chemistry (Scheme 1). Compound **6f** (Figure 2) was the most active (IC_{50} value from 6.8–10.4 μM) and was more active than the standard drug cisplatin on HT-29 cells. Aminonaphthoquinone–1,2,3–triazole hybrids produced some activity but the activity was highly influenced by the substituent present in the terminal phenyl ring. The presence of a strong electron-withdrawing group in the *para* position of the ring (4-(trifluoromethyl)benzyl moiety in compound **6f**) greatly enhanced its activity.[66]

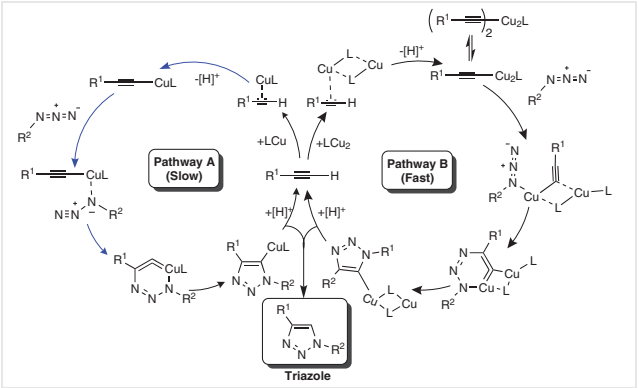

Figure 1 Two competitive pathways for the CuAAC-catalyzed click reaction by a mononuclear Cu species (Pathway A) and by a dinuclear Cu catalyst (Pathway B)[65]

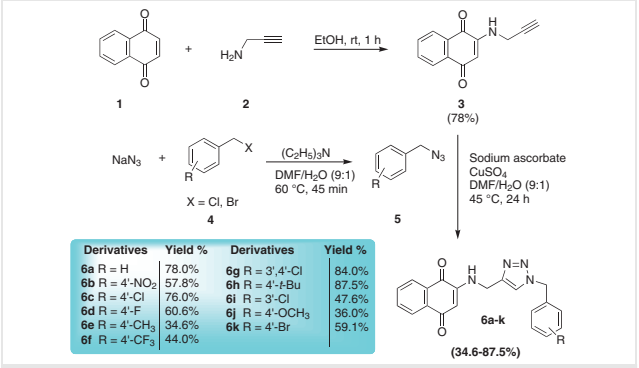

Scheme 1 Synthesis of triazole-based naphthalene-1,4-diones[66]

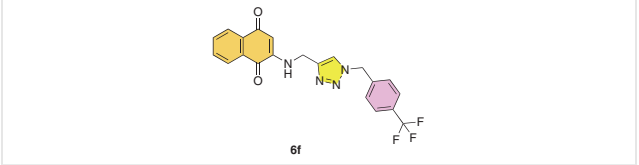

Figure 2 Structure of triazole-based naphthalene-1,4-dione compound **6f**[66]

Through the use of click chemistry and copper(I) oxide nanoparticles, melampomagnolide B–triazole conjugates were produced (Scheme 2) and were then tested for their anticancer activity on U87, A549, PANC1, HCT116, and Bel7402 cells. Compound **6e** (Figure 3) was most active with an IC_{50} value of 0.43 μM on HCT116 cells. A copper-catalyzed click reaction of alkyne and azide produced melampomagnolide B–triazole conjugates and their activity was higher than melampomagnolide B (MMB); the anticancer activity was increased by the presence of electron with-

drawing groups such as nitro- or fluorine. These induced apoptosis and inhibited proliferation and migration of HCT116 cells.[67]

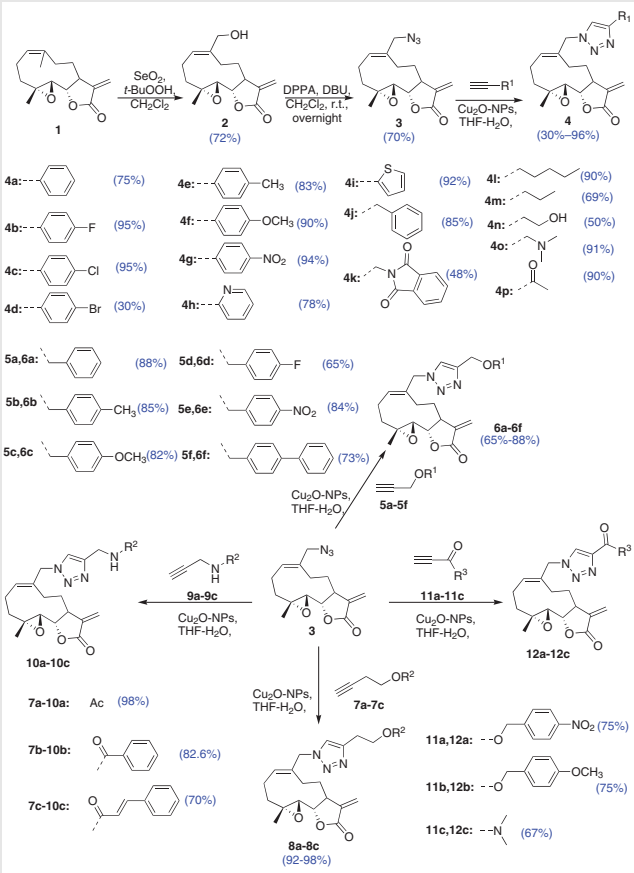

Scheme 2 Synthesis of melampomagnolide B–triazole conjugates[67]

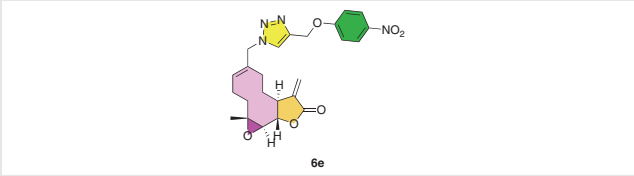

Figure 3 Structure of melampomagnolide B–triazole conjugate **6e**[67]

1,2,3-Triazole-containing dehydroabietic acids (DHAA), synthesized using click chemistry (Scheme 3) were tested for anticancer activity on MCF7, MDA-MB-231, PC-3, and SKOV-3 cells. Compound **23** (Figure 4) was found to be the most active (IC_{50} values ranging from 0.7–1.2 μM) with higher toxicity toward cancer cells than the normal cells. Modified DHAA compounds with methoxy substitution at the terminal benzene ring were highly active. The compounds with 3-acetamide and 3-*tert*-butyl carbamate substitution at benzene ring were the most active, which confirms that the activity was highly dependent on the substitution at the benzene ring.[68]

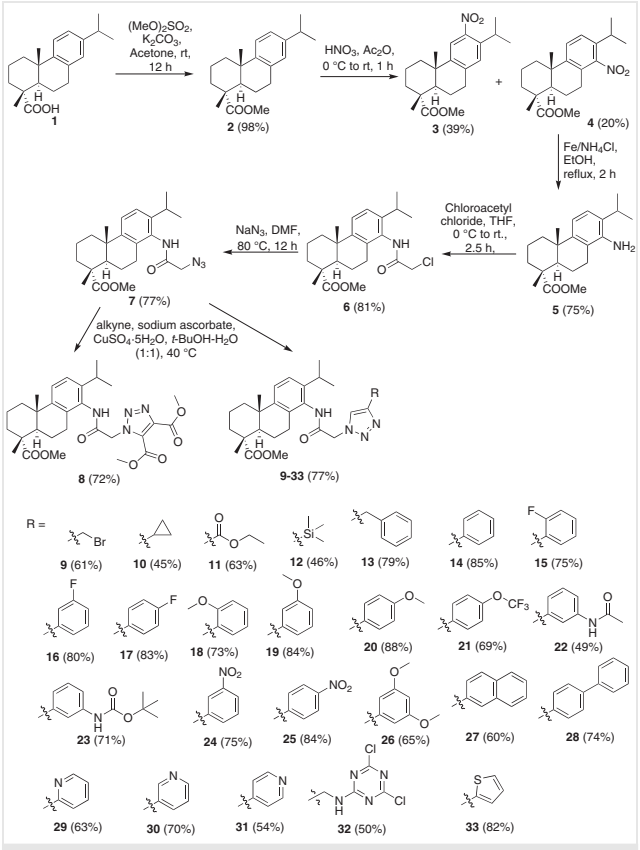

Scheme 3 Synthesis of 1,2,3-triazole-containing dehydroabietic acids[68]

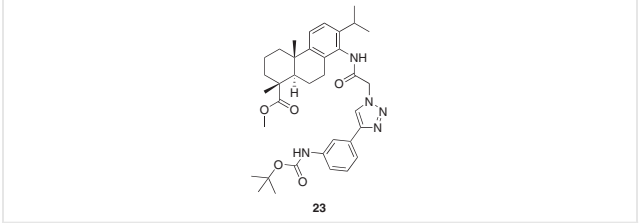

Figure 4 Structure of 1,2,3-triazole-containing dehydroabietic acid compound **23**[68]

1,2,3-Triazole-based thienopyrimidine conjugates containing various sugar moieties were synthesized (Scheme 4) using Cu(I)-catalyzed click chemistry. The compounds were then tested for their cytotoxic activity on MCF-7 and HCT-116 cells. Compounds **10** and **12** (Figure 5) were found to be the most active. Though none of the compounds were as active as doxorubicin on HCT-116 cells all the compounds were more active than doxorubicin against MCF-7 cells. Compounds **7**–**12** produced good EGFR inhibition, better than the standard drug gefitinib.[69]

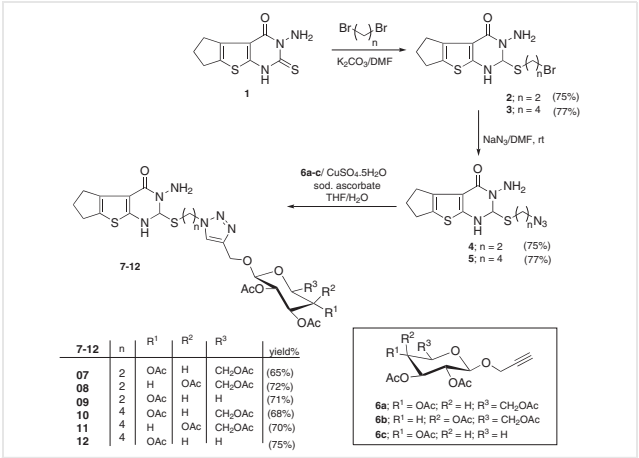

7-12	n	R^1	R^2	R^3	yield%
07	2	OAc	H	CH_2OAc	(65%)
08	2	H	OAc	CH_2OAc	(72%)
09	2	OAc	H	H	(71%)
10	4	OAc	H	CH_2OAc	(68%)
11	4	H	OAc	CH_2OAc	(70%)
12	4	OAc	H	H	(75%)

Scheme 4 Synthesis of sugar-containing 1,2,3-triazole-based thienopyrimidine conjugates[69]

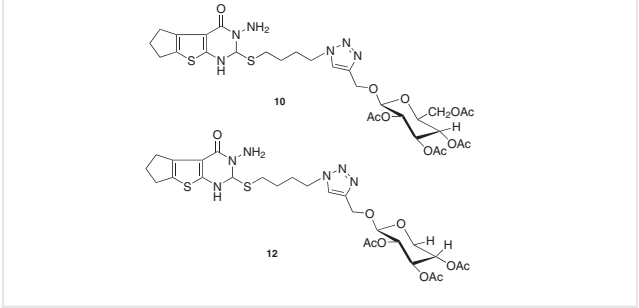

Figure 5 Structure of sugar-containing 1,2,3-triazole-based thienopyrimidine conjugates **10** and **12**[69]

The terminal acetylenic thienopyrimidine derivatives, which lack the sugar component, were the most effective molecules. Higher activity was seen in thienopyrimidine systems based on 1,2,3-triazole glycosides and containing a linker with four methylene (CH_2) groups. Glycosyl-1,2,3-triazole derivatives of the thienopyrimidine system with cyclic glucopyranosyl unit, either acetylated or free hydroxyl moiety, were found to be more effective against the HCT-116 cell line. In comparison to its gluco- and galactopyranosyl counterparts, glycosyl-1,2,3-triazole **12** containing the xylopyranosyl moiety exhibited significantly stronger cytotoxic activity against the MCF-7 cancer cell lines.[69]

Toradol (Ketorolac) was modified to boost its cell permeability and anticancer activity by using click chemistry to synthesize its 1,2,3-triazolyl ester **3** (Scheme 5). The resulting compound **3** was 500 times more active than the parent compound (Toradol) with an IC_{50} value of 24 nM against PKA1-growth-dependent A549 cells. It inhibited PKA1 with an IC_{50} value of 65 nM and COX-2 with an IC_{50} of 6 nM. The activity of the compound was 5000-fold more potent on PAK1-growth-dependent B16F10 cells. The permeability was boosted 10 times compared to the parent molecule.[70]

Curcumin pyrazole derivatives were synthesized using click chemistry (Scheme 6). These compounds were then tested for their anticancer potential on UM-SCC-74A and CAL27 cells and also studied on pAKT, pERK1/2, pFAK, and pSTAT3 for mechanism determination. Compounds **2** and **5** (Figure 6) were found to be highly active against CAL27 cells and efficiently inhibited pSTAT3 phosphorylation.[71]

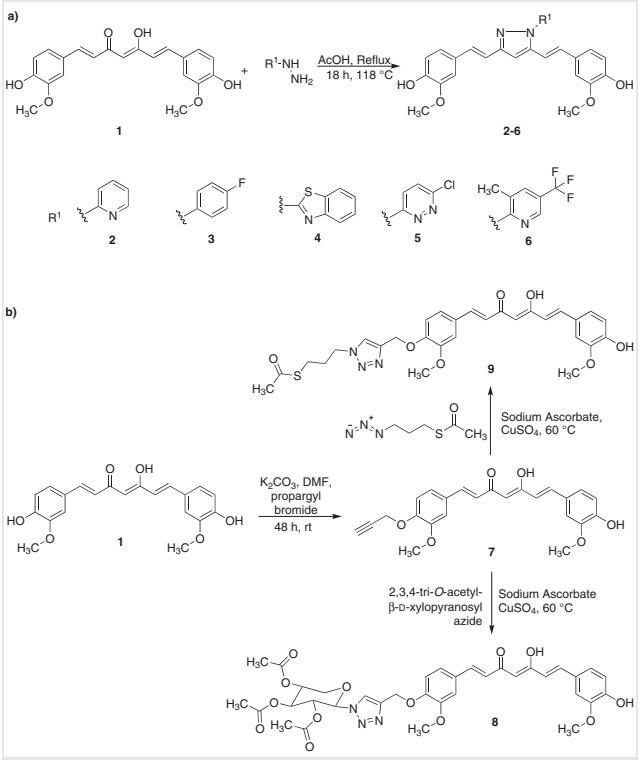

Scheme 6 Synthesis of curcumin-based derivatives[71]

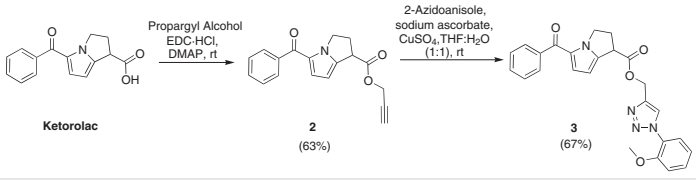

Scheme 5 Synthesis of the 1,2,3-triazolyl ester of Toradol (Ketorolac)[70]

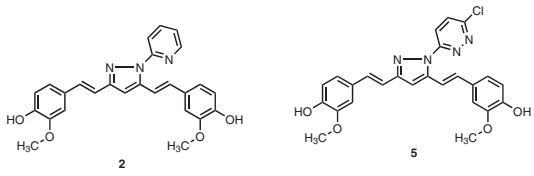

Figure 6 Structure of curcumin-based derivative compounds **2** and **5**[71]

Sodium azide, aralkyl halides, 4-hydroxycarbazole, malononitrile, and *N*-propargyl isatins reacted in the presence of Cell-CuI NPs (cellulose-supported CuI-nanoparticles) to form 1,2,3-triazole-tethered spirochromenocarbazoles in a one-pot synthesis reaction (Scheme 7). The synthesized compounds were tested for their anticancer activity on THP-1, A-549, PANC-1, HeLa, MDA-MB-231, and MCF-7. Many compounds produced good anticancer activity against HeLa, MCF-7, and MDA-MB-231 cells (IC_{50} value < 10 μM). Compound **6f** (Figure 7) (IC_{50} = 2.13 μM) was most active on MCF-7 cells, compound **6k** (Figure 7) (IC_{50} = 3.78 μM) on MDA-MB-231, and compound **6u** (Figure 7) (IC_{50} = 3.5 μM) on HeLa cells. All the compounds were nontoxic to HUVACs and induced cell death by apoptosis. *N*-Propargyl isatin and 5-bromo-*N*-propargyl isatin are the sources of most active molecules, although the substitution of chloro, fluoro, or methyl group on *N*-propargyl isatin has little impact on the anticancer activity. Benzyl bromides possessing electron-withdrawing groups were shown to be more potent than other compounds.[72]

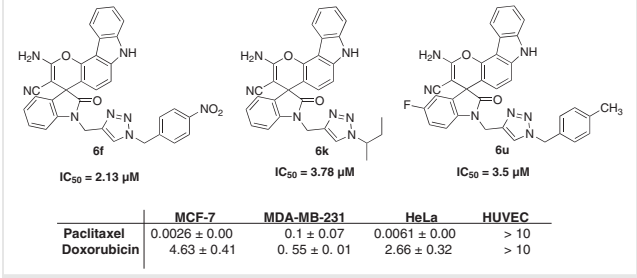

	MCF-7	MDA-MB-231	HeLa	HUVEC
Paclitaxel	0.0026 ± 0.00	0.1 ± 0.07	0.0061 ± 0.00	> 10
Doxorubicin	4.63 ± 0.41	0. 55 ± 0. 01	2.66 ± 0.32	> 10

Figure 7 Structure of 1,2,3-triazole-tethered spirochromenocarbazoles compounds **6f**, **6k**, and **6u**[72]

4β-Amidopodophyllotoxin conjugates containing triazoles were synthesized exploiting click chemistry (Scheme 8) and tested for anticancer activity on MCF-7, HT29, B16, and HeLa cells. No compound was as active as the standard drugs etoposide and podophyllotoxin on B16 cells, compound **5j** (Figure 8) was most active on the remaining three cell lines (IC_{50} = 0.07 μM on HeLa cells, 0.1 μM on HT29, and 0.91 μM on MCF-7 cells) and was more active than both the standard drugs. The compounds increased the caspase-3 levels, arrested the cell cycle in the G2/M phase, and produced apoptosis. The compounds produced good tubulin inhibition in the *in vitro* studies and bound to colchicine site in the *in silico* studies. It was clear from the *in vitro* studies that in triazolo-linked podophyllotoxins, the compound containing triazole ring substituted with 4-bromophenyl **5j** was most active. It was clear from the molecular docking studies that oxygen and nitrogen from the amide and the bromine-substituted phenyl ring established hydrogen bonds with tubulin. π-Stacking was observed in

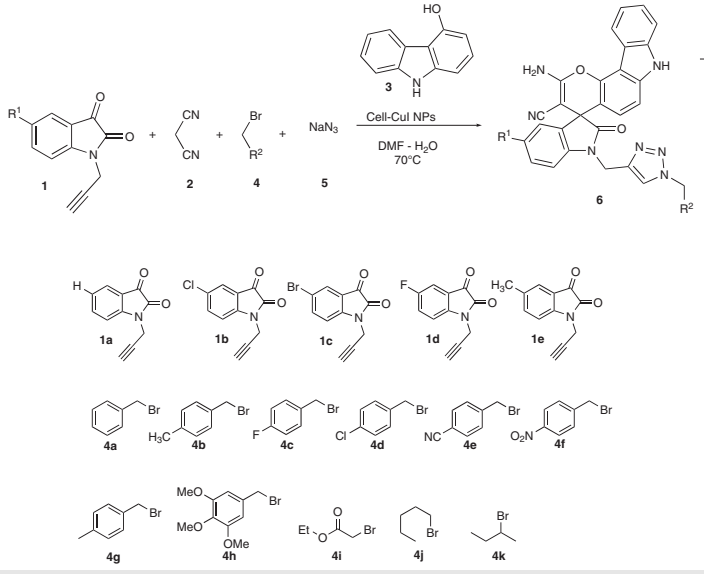

Compound	*N*-propargyl isatin	Aralkyl or alkyl bromide	Y%
6a	1a	4a	92
6b	1a	4b	90
6c	1a	4c	87
6d	1a	4d	89
6e	1a	4e	84
6f	1a	4f	87
6g	1a	4g	85
6h	1a	4h	83
6i	1a	4i	91
6j	1a	4j	86
6k	1a	4k	84
6l	1b	4a	92
6m	1b	4b	87
6n	1b	4c	89
6o	1b	4d	90
6p	1c	4a	85
6q	1c	4b	87
6r	1c	4c	88
6s	1c	4d	86
6t	1d	4a	87
6u	1d	4b	85
6v	1d	4c	83
6w	1d	4d	81
6x	1e	4a	88
6y	1e	4b	86
6z	1e	4c	89
6aa	1e	4d	84

Scheme 7 Synthesis of 1,2,3-triazole-tethered spirochromenocarbazoles[72]

the case of the triazole ring, the phenyl ring with trimethoxy substituents, and phenyl rings with bromine substituents.[73]

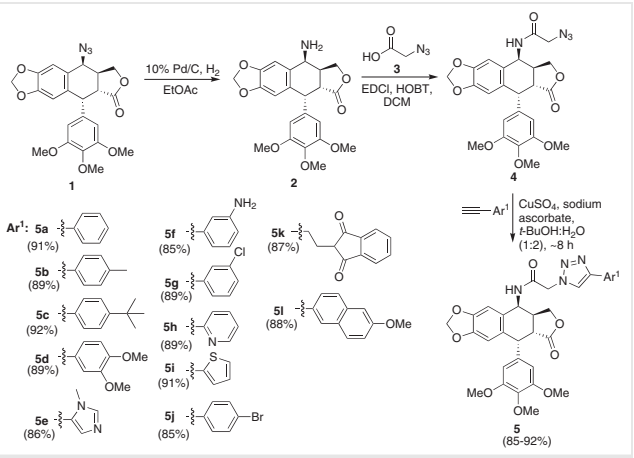

Scheme 8 Synthesis of triazole-containing 4β-amidopodophyllotoxin conjugates[73]

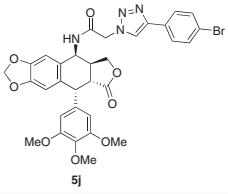

Figure 8 Structure of triazole-containing 4β-amidopodophyllotoxin conjugate **5j**[73]

Triazole-containing analogues of DDO-6101 (**3**), a caged xanthone, were prepared by click chemistry (Scheme 9) to improve the anticancer activity in *in vivo* studies and the druglike properties were tested for their anticancer activities on U2OS, HCT116, HepG2, and A549 cells.[74] There was no reduction in the cytotoxicity and the compounds were even active against cisplatin and taxol-resistant A549 cells.

Compound DDO-6318 (**8g**) (Figure 9) with the best anticancer activity in most of the cases and good druglike properties was considered for *in vivo* studies and turned out to be much more potent than the original DDO-6101 (**3**). The cytotoxic action of xanthones may be increased by adding a triazole moiety with nitrogen-containing hydrophilic groups, particularly morpholino and 4-methylpiperizin-1-yl groups, but the length of the alkyl chain imposed no significant change in the activity.[74]

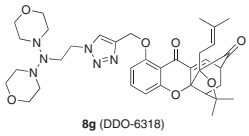

Figure 9 Structure of a triazole-containing analogue of DDO-6101, compound **8g** (DDO-6318)[74]

1,2,3-Triazole-containing pyrrolobenzodiazepines **1** and **2** synthesized via click chemistry using microwave irradiation and catalysis by Cu(I) (Scheme 10) were tested for percent growth inhibition at 10^{-5} M concentration on various cancer cell lines. Most compounds produced moderate activity, compound **1c** (Figure 10) produced the highest percent inhibition of 43.45% at the concentration of 10^{-5} M. Two sets of pyrrolobenzodiazepine-triazole derivatives **1** and **2** were synthesized, the former containing simple substituted phenyl attached to triazole and latter containing a 2-oxo-2-(substituted phenylamino)ethyl. Compound **1c** was most active on SNB-75, suggesting that the compound containing a simple 2-chlorophenyl substituent on triazole ring produced best activity against SNB-75.[75]

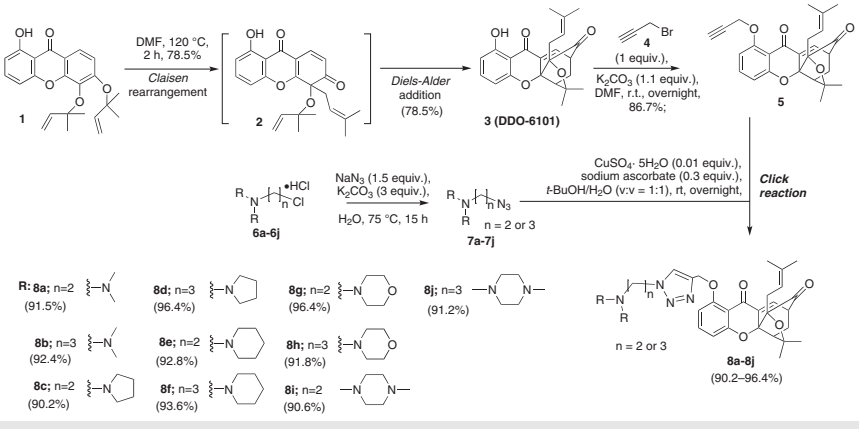

Scheme 9 Synthesis of triazole-containing analogues of DDO-6101[74]

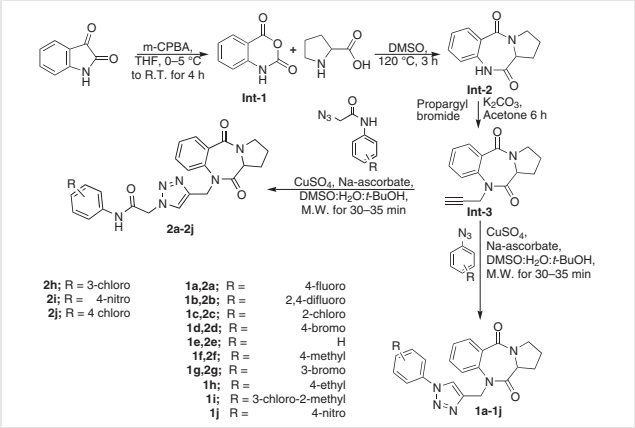

Scheme 10 Synthesis of 1,2,3-triazole-containing pyrrolobenzodiazepines[75]

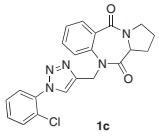

Figure 10 Structure of 1,2,3-triazole-containing pyrrolobenzodiazepine compound **1c**[75]

Triazole derivatives of D-(+)-pinitol with substitutions at N1 and C4 of the triazole were synthesized by a copper(I) catalysis (Scheme 11) and were tested for anticancer activity on Mia-Paca-2, HCT116, and HL-60 cells. Compound **7** (Figure 11) was the most active on Mia-Paca-2 (IC_{50} value 16.4 μM), compound **3** (Figure 11) on HCT116 (IC_{50} value 17.5 μM), and compound **2** (Figure 11) on HL-60 (IC_{50} value 19.2 μM) cells. Methyl, nitro, and bromo groups on the phenyl ring at N1 of the imidazole produced better cytotoxic agents.[76]

N-((1-((1*H*-Benzo[*d*]imidazol-2-yl)methyl)-1*H*-1,2,3-triazol-4-yl)methyl)aniline derivatives **7** were synthesized by click chemistry in a one-pot synthesis (Scheme 12) and were then tested for their anticancer activity on NCI-60 cells. Compound **7e** (Figure 12) with 70% growth inhibition of UO-31 cells at a concentration of 10 μM was most active.[77]

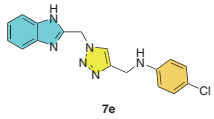

Figure 12 Structure of compound **7e**[77]

The synthesis of triazole-benzimidazole-chalcones **10** and **11** was performed using click chemistry (Scheme 13) and the compounds were tested for anticancer activity with PC3, MDA-MB-231, and T47-D cells. Though no compound was as active as doxorubicin (the standard drug), compound **10d** (Figure 13) with IC_{50} values of 5.89 μM and 6.23 μM was most active on MDA-MB-231 and T47-D, respectively. Compound **10h** (Figure 13) with an IC_{50} value of 5.64 μM was most active on PC3 cells. More activity was produced by the benzyl-linked 1,2,3-triazole group.[78]

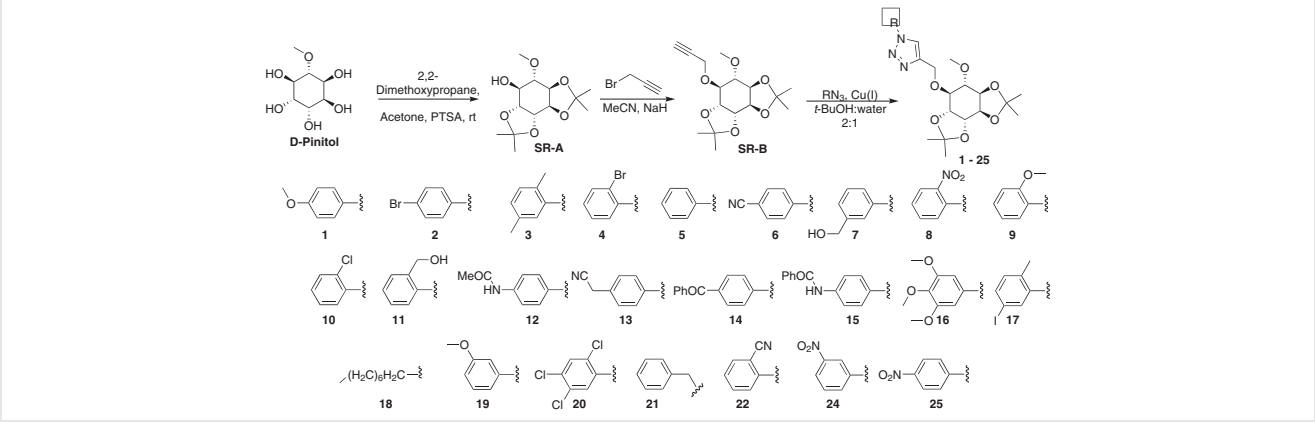

Scheme 11 Triazole derivatives of D-(+)-pinitol[76]

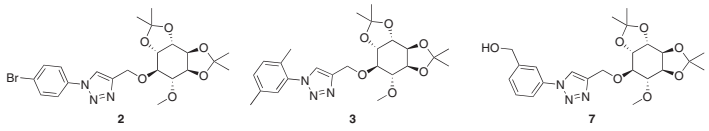

Figure 11 Structure of triazole derivatives of D-(+)-pinitol compounds **2**, **3**, and **7**[76]

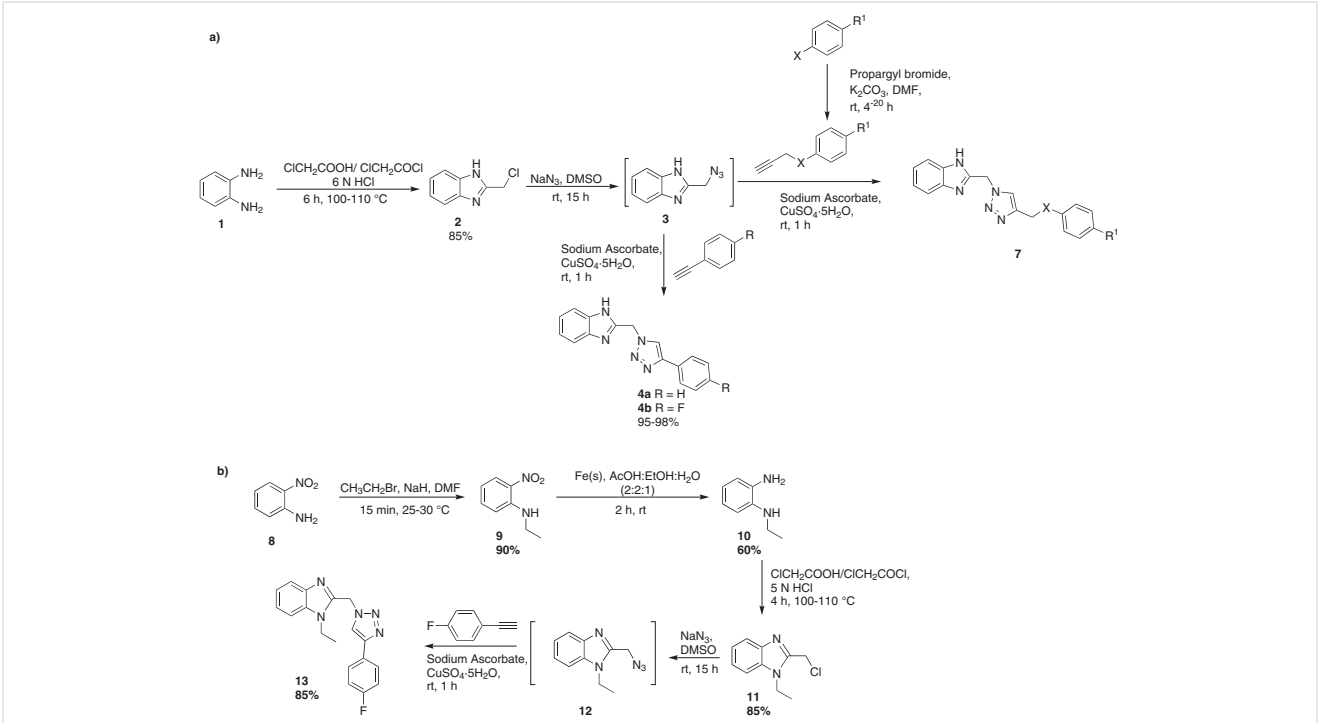

Scheme 12 (a) Synthesis of *N*-((1-((1*H*-benzo[*d*]imidazol-2-yl)methyl)-1*H*-1,2,3-triazol-4-yl)methyl)aniline and 2-((4-phenyl-1*H*-1,2,3-triazol-1-yl)methyl)-1*H*-benzo[*d*]imidazole derivatives; (b) synthesis of 1-ethyl-2-((4-(4-fluorophenyl)-1*H*-1,2,3-triazol-1-yl)methyl)-1*H*-benzo[*d*]imidazole[77]

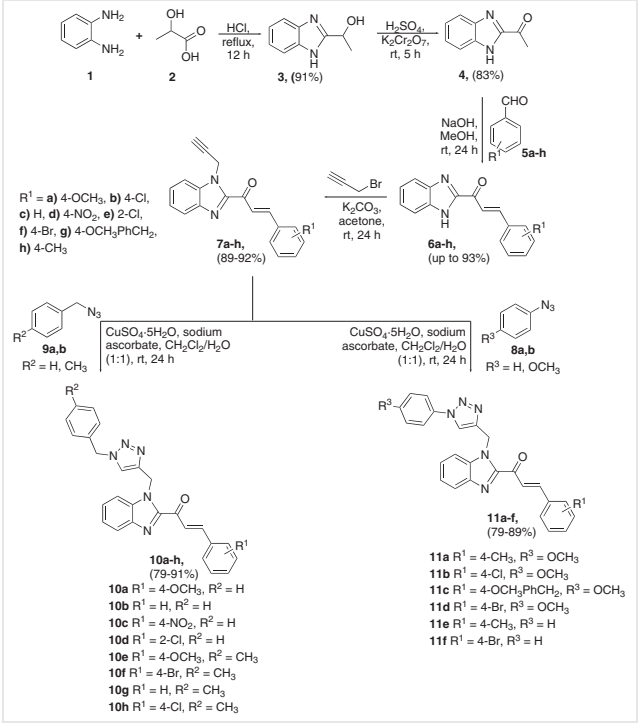

Scheme 13 Synthesis of triazole-benzimidazole-chalcones[78]

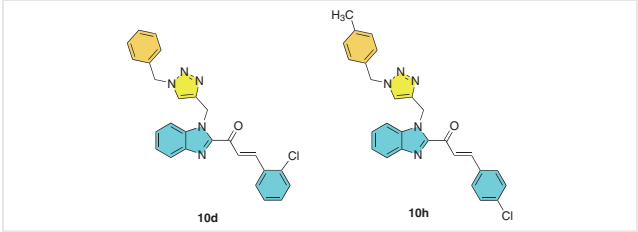

Figure 13 Structure of triazole-benzimidazole-chalcones **10d** and **10h**[78]

1,2-Isoxazole-xanthenedione **12**, 1,2-isoxazole-acridinedione **11**, 1,2,3-triazole-xanthenedione **10**, and 1,2,3-triazole-acridinedione hybrids **9** synthesized via click chemistry (Scheme 14) were tested for anticancer activity on PC3, MDA-MB-231, and T47-D cells. Though none of the compounds was as active as the standard drug doxorubicin, compound **10c** (IC_{50} of 10.20 μM, 20.88 μM and 14.50 μM on PC3, MDA-MB-231, and T47-D cells, respectively) was most active among all the synthesized compounds. By adding 1,2-isoxazole to the acridine scaffold, cytotoxicity in metastatic cancer could be boosted in 1,2-isoxazole/1,2,3-triazole-xanthenedione/acridinediones. Among the most active hybrids *O*-1,2,3-triazole-xanthenediones containing unsubstituted aromatic rings were most cytotoxic. The 1,2,3-triazole's orthogonal position at the xanthenedione scaffold promotes cytotoxicity in PC3. Conjugation and position of the isoxazole moiety at the acridinedione scaffold

are in favor of an increased cytotoxicity. Compounds sharing acridine/xanthene have resulted in promising antiproliferative activity against a panel of tested cancer cells. Acridine-1,2,4-triazole compounds with different substitutions at the *para* position of the phenyl ring exhibited the most potent anticancer activity against MCF-7, HT-29, A-549, and A-375. Acridine-thiophene hybrids show selectivity toward HCT-116 cells.[79]

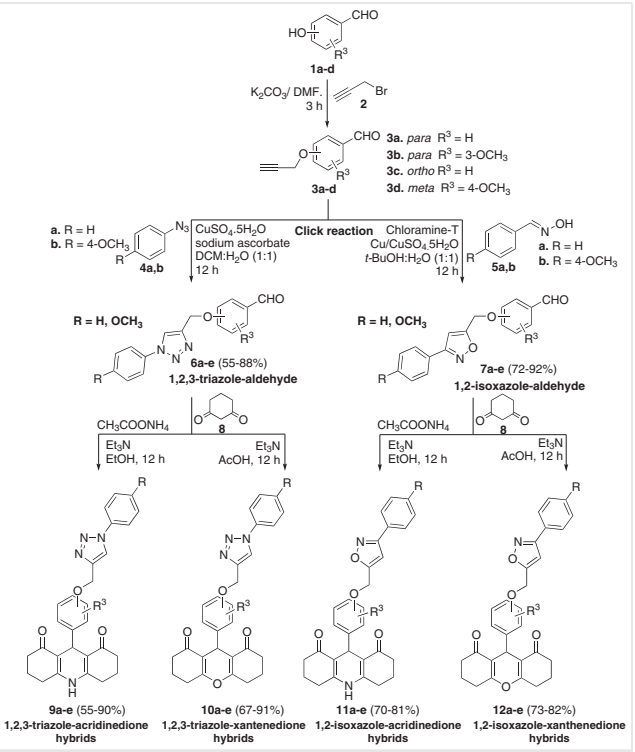

Scheme 14 Synthesis of 1,2-isoxazole-xanthenedione/acridinedione and 1,2,3-triazole-xanthenedione/acridinedione hybrids[79]

Ludartin 1,4-disubstituted-1,2,3-triazoles **3** were synthesized using click chemistry (Scheme 15) and tested for anticancer activity on MCF-7, HCT-116, PC-3, A-549, and T98G cells. Though compound **3q** (Figure 14) with 3,4-dimethyl substitution was highly active among the synthesized compounds, it was not as active as the parent ludartin.[80]

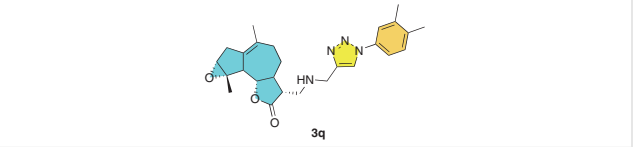

Figure 14 Structure of ludartin 1,4-disubstituted-1,2,3-triazole compound **3q**[80]

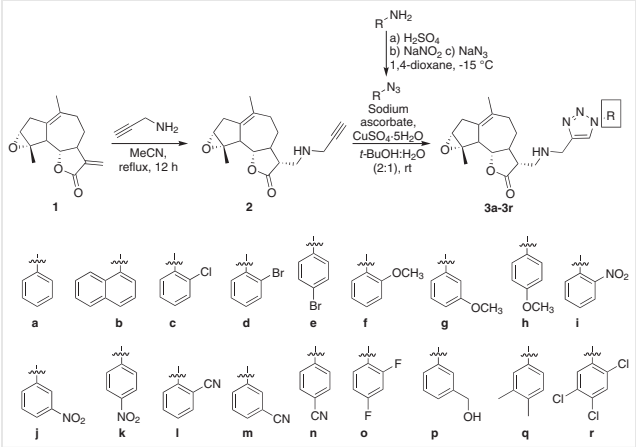

Scheme 15 Synthesis of ludartin 1,4-disubstituted-1,2,3-triazoles[80]

6-(4-((Substituted-1*H*-1,2,3-triazol-4-yl)methyl)piperazin-1-yl)phenanthridines were synthesized **7** (Scheme 16) using Cu(I)-catalyzed click chemistry and tested for anticancer activity on HL60, U937, COLO205, and THP1 cells. Among the synthesized compounds, **7g** (Figure 15) (IC_{50} = 9.73 μM) was most active on THP1 cells but was not as active as the standard drug etoposide. Compound **7h** (Figure 15) was highly active on HL60 cells (IC_{50} = 7.22 μM) and was more active than the standard drug.[81]

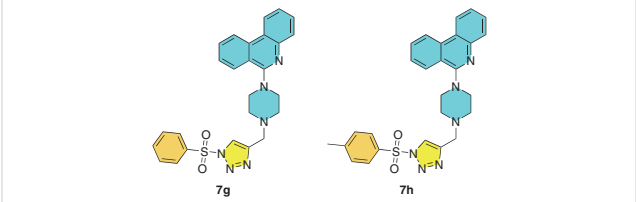

Figure 15 Structures of 6-(4-((substituted-1*H*-1,2,3-triazol-4-yl)methyl)piperazin-1-yl)phenanthridine compound **7g** and **7h**[81]

Osthol-based triazole compounds **3–22** were synthesized where the open lactone ring was exploited for the addition of a triazole via click chemistry (Scheme 17). The synthesized compounds proved to be more active than osthol on A-431, PC-3, A549, NCI-H322, T47D, HCT-116, and colo-205 cells. Compound **8** (Figure 16) was most active against A-431, T47D, HCT-116, and Colo-205 cells with IC_{50} values of 7.2 μM, 3.6 μM, 4.9 μM, and 1.3 μM, respectively, more active than the standard drug against T47D and A-431 cells, but not as active in case of Colo-205 and HCT-116. Compound **11** (Figure 16) was most active on PC3 cells with an IC_{50} value of 14.2 μM and compound **20** (Figure 16) on NCI-H322 cells (IC_{50} value 14.4 μM) but they were not as active as the standard drug BEZ-235. Compound **14** (Figure 16) (IC_{50} = 2.2 μM) was most active on A549 cells and its activity was better than the standard drug.[82]

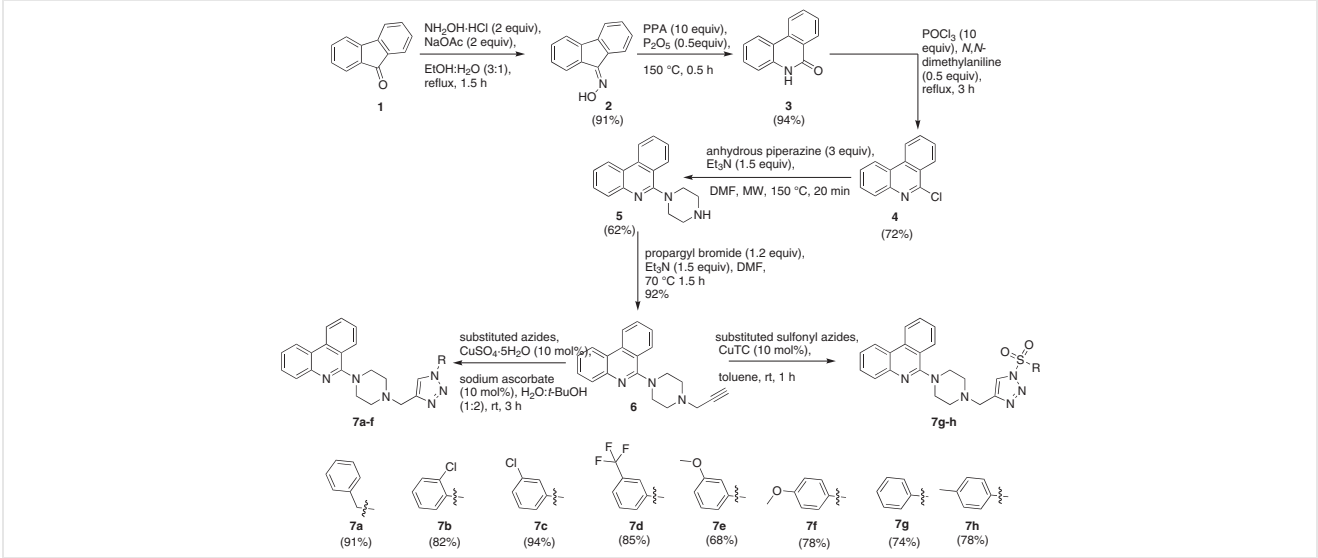

Scheme 16 Synthesis of 6-(4-((substituted-1*H*-1,2,3-triazol-4-yl)methyl)piperazin-1-yl)phenanthridines[81]

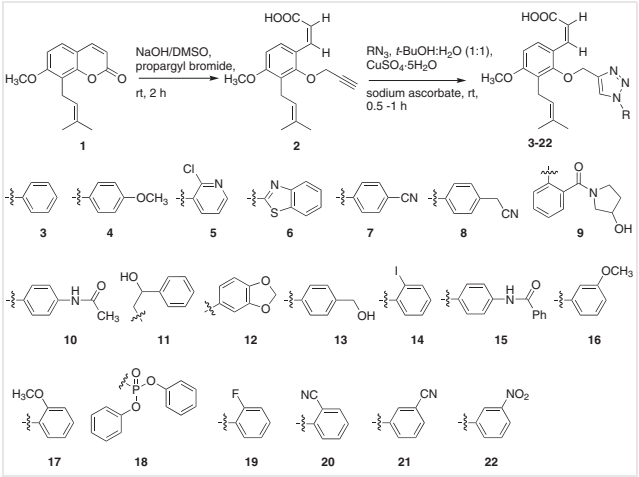

Scheme 17 Synthesis of osthol-based triazole compounds[82]

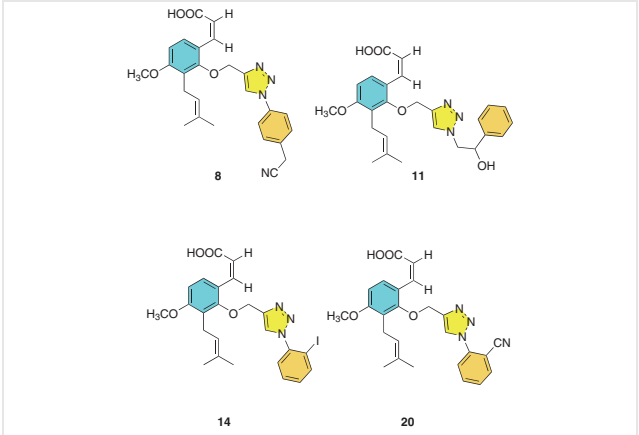

Figure 16 Structure of osthol-based triazole compounds **8**, **11**, **14**, and **20**[82]

Dihydroartemisinin-coumarin hybrids **10**–**13** (Scheme 18), synthesized using click chemistry, were tested for their anticancer activity on HT-29, MDA-MB-231, and HCT-116 cells under anoxic and normoxic conditions. The hybrids produced moderate activity with IC_{50} value from 0.05 to 125.40 μM. The compounds were more active on HT-29 cells in anoxic conditions. The cytotoxicity in most of the compounds was found to be greater in anoxic conditions than in normoxic. Compounds **10a**–**e** were more active on HT-29 cells.[83]

Pyrazolyl–chalcone hybrids were synthesized using triazole click chemistry (Scheme 19) and were then tested for their anticancer activity on A-549, COLO-205, and THP cells. Compound JGPT-6 and JGPT-11 (Figure 17) were found to be very active with JGPT-6 being most active on COLO-205 cells (99% inhibition at 100 μM) whereas compound JGPT-11 was most active on THP and A-549 cells with 95% A-549 inhibition at a concentration of 100 μM and 79% of THP at the same concentration. Cytotoxicity is noticeably reduced when deactivating groups like Br and Cl are present. The methoxy groups significantly increased cytotoxicity.[84]

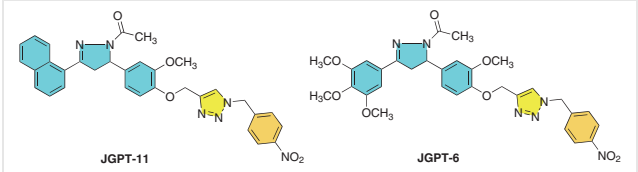

Figure 17 Structure of pyrazolyl–chalcone hybrids JGPT-6 and JGPT-11[84]

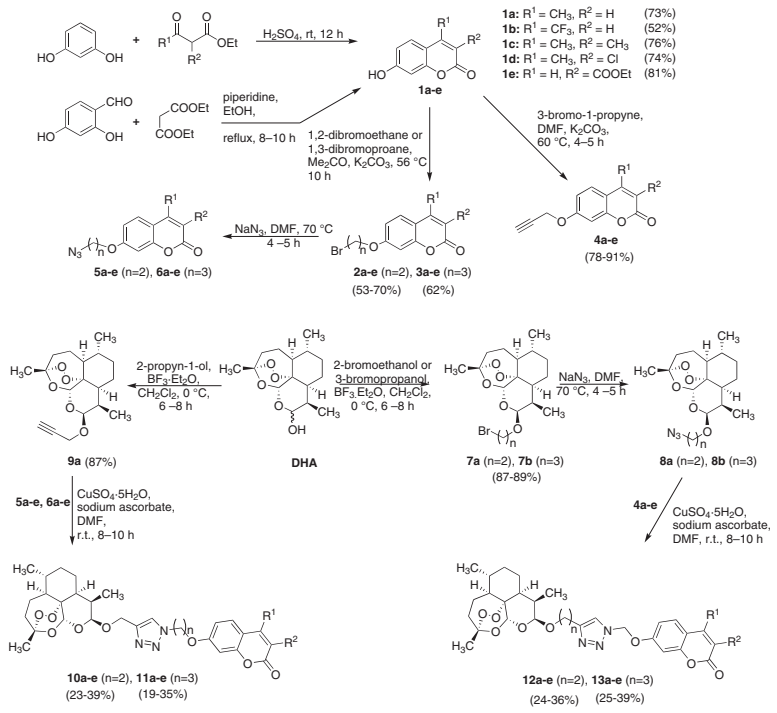

Scheme 18 Synthesis of dihydroartemisinin–coumarin hybrids[83]

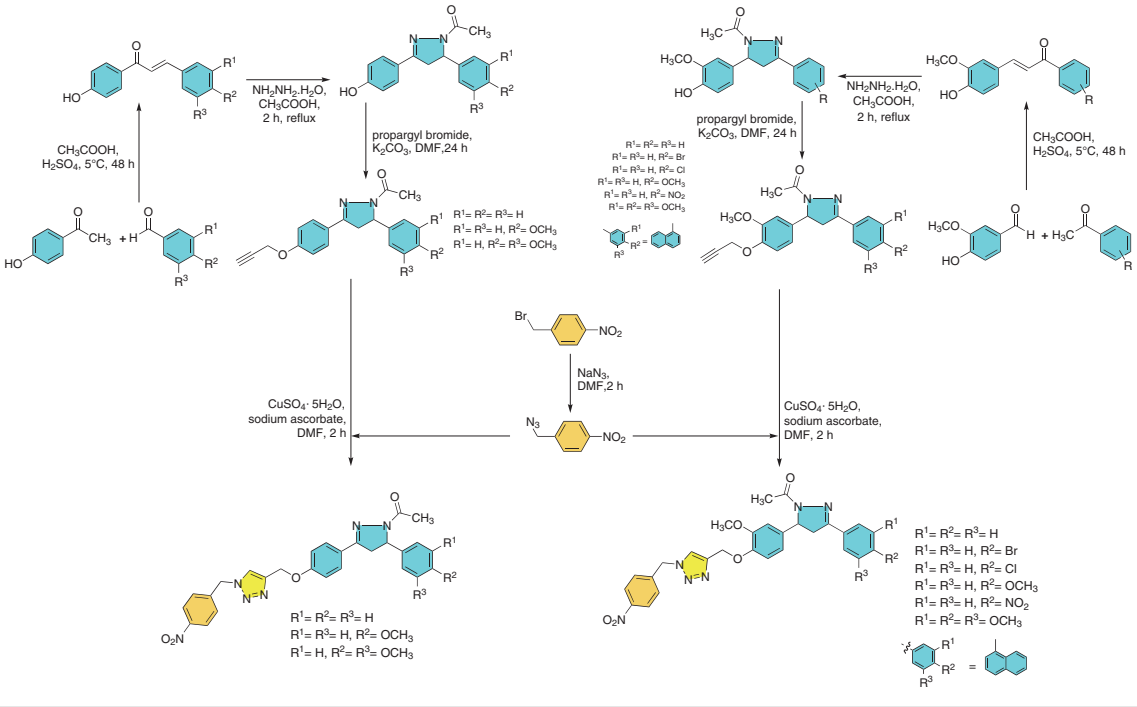

Scheme 19 Synthesis of pyrazolyl–chalcone hybrids[84]

Triazole-mansonone E derivatives **12** with halogen substitution at C-9 were synthesized by click chemistry (Scheme 20). The derivatives produced potent topoisomerase inhibition (both in Topo I and Topo II). The compounds were also tested for their activity on HeLa, K562, HL-60, and A549 cells. None of the compounds were as active as the standard drug etoposide on HL-60 cells, but many compounds were more active than etoposide on HeLa, K562, and A549 cells. Compound **12a-10** (Figure 18) (IC_{50} = 11.38 μM) was most active on A549 cells whereas compound **12b-9** (Figure 18) on K562 and **12b-11** (Figure 18) on HeLa with IC_{50} values of 2.82 μM and 7.72 μM, respectively. These compounds (**12a-10**, **12b-9**, and **12b-11**) (Figure 18) were more active than the standard except for compound **12b-9** (Figure 18) with an IC_{50} value of 1.49 μM on HL-60 cells. The anticancer efficacy of triazole-mansonone E derivatives was impacted by a variety of situations. The first is the C-9 substituent, where bromo was more efficient than chloro. In comparison to cyclopropyl, carboxylic acid ethyl ester, and carboxylic acid methyl ester, aromatic substituents have better activity when present on triazoles. Longer alkyl chains boosted activity, while alkyl substituents at position 4 of the phenyl ring provided better activity.[85]

Triazole-based isosteviol compounds **12** and **13** were synthesized using click chemistry (Scheme 21) and were tested on HeLa, HCT116, PC-3, MDA231, ASPC-1, A549, HL-60, and MOLT-4 cells for their anticancer activity. Compound **12a** (Scheme 21) was most active on all cell lines except HeLa cells with IC_{50} values ranging from 4.79–28.8 μM. Compound **12a** produced the lowest IC_{50} for ASPC-1 and which was 4.79 μM. Compound **12b** (Scheme 21) was highly active on HeLa cells (IC_{50} = 5.83 μM) and was highly specific for HeLa, MOLT-4, and HCT116 cells. In the case of triazole-based isosteviol the linker between the triazole and benzene ring was an important factor in the cytotoxic activity of the isosteviol carboxylic group modified conjugates. The aliphatic linker between the triazole and benzene rings with a polar methoxycarbonyl group decreased activity. When the polarity of the triazole-containing moiety increases, the anticancer activity of isosteviol conjugates decreases noticeably. Moreover, the capacity of isosteviol conjugates to inhibit the growth of cancer cells depends on the triazole moiety's hydrophobicity.[86]

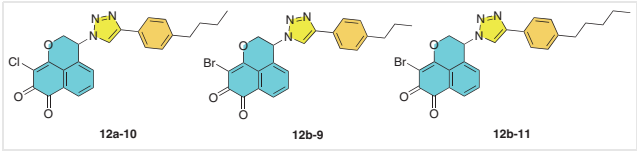

Figure 18 Structure of triazole mansonone E derivatives **12a-10**, **12b-9**, and **12b-11**[85]

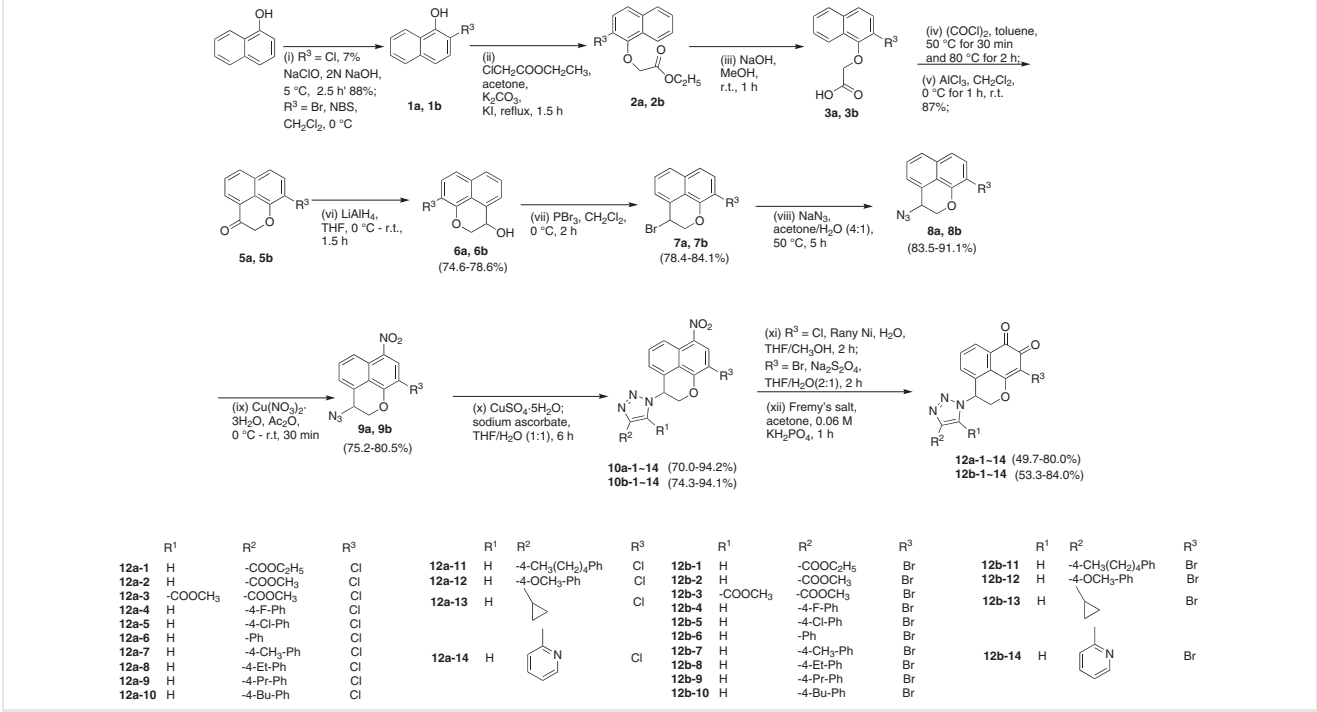

	R1	R2	R3
12a-1	H	-$COOC_2H_5$	Cl
12a-2	H	-$COOCH_3$	Cl
12a-3	-$COOCH_3$	-$COOCH_3$	Cl
12a-4	H	-4-F-Ph	Cl
12a-5	H	-4-Cl-Ph	Cl
12a-6	H	-Ph	Cl
12a-7	H	-4-CH_3-Ph	Cl
12a-8	H	-4-Et-Ph	Cl
12a-9	H	-4-Pr-Ph	Cl
12a-10	H	-4-Bu-Ph	Cl

	R1	R2	R3
12a-11	H	-4-$CH_3(CH_2)_4$Ph	Cl
12a-12	H	-4-OCH_3-Ph	Cl
12a-13	H		Cl
12a-14	H		Cl

	R1	R2	R3
12b-1	H	-$COOC_2H_5$	Br
12b-2	H	-$COOCH_3$	Br
12b-3	-$COOCH_3$	-$COOCH_3$	Br
12b-4	H	-4-F-Ph	Br
12b-5	H	-4-Cl-Ph	Br
12b-6	H	-Ph	Br
12b-7	H	-4-CH_3-Ph	Br
12b-8	H	-4-Et-Ph	Br
12b-9	H	-4-Pr-Ph	Br
12b-10	H	-4-Bu-Ph	Br

	R1	R2	R3
12b-11	H	-4-$CH_3(CH_2)_4$Ph	Br
12b-12	H	-4-OCH_3-Ph	Br
12b-13	H		Br
12b-14	H		Br

Scheme 20 Synthesis of triazole–mansonone E derivatives[85]

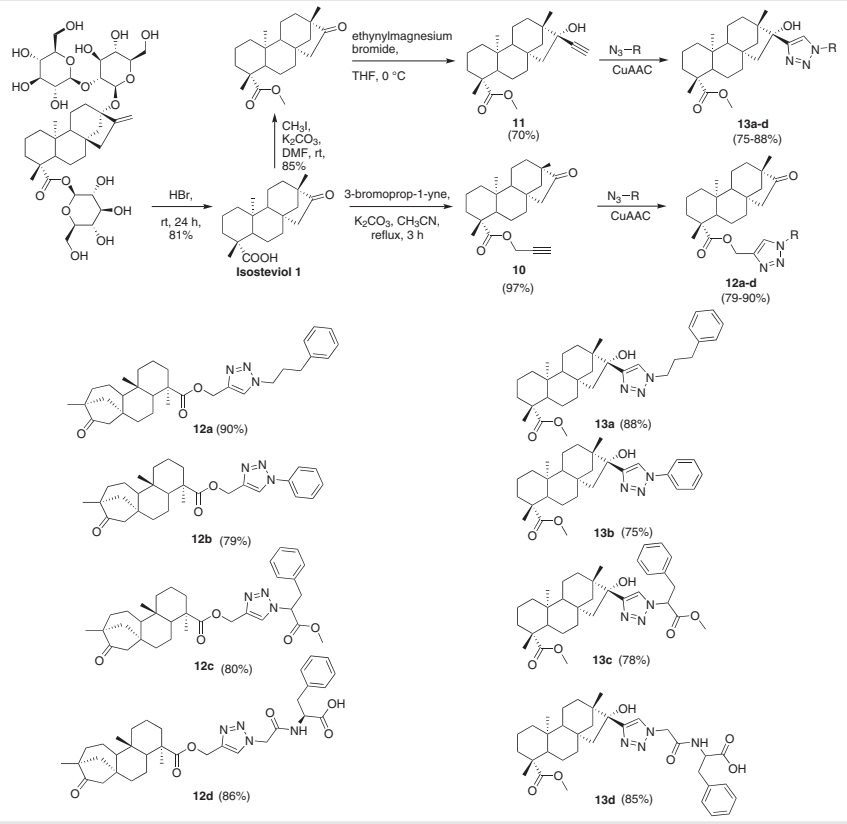

Scheme 21 Synthesis of triazole-based isosteviol compounds[86]

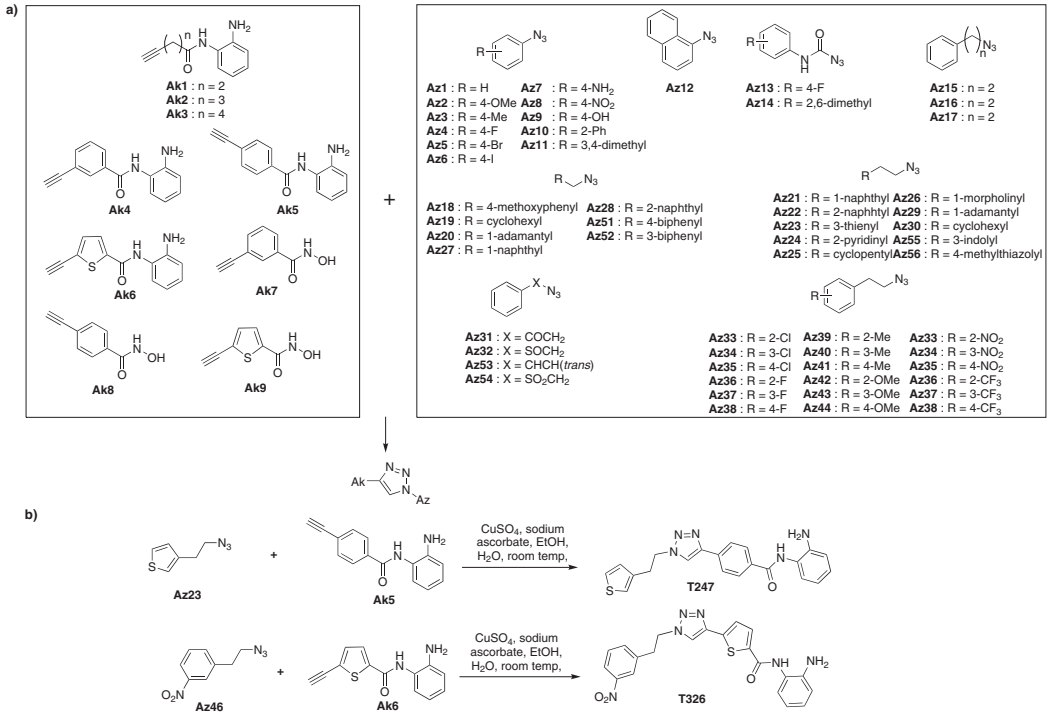

Scheme 22 (a) General alkyne and azide precursors; (b) synthesis of compounds **T247** and **T326**[87]

Triazole-based compounds were synthesized using azide-alkyne click chemistry (Scheme 22) as potential HDAC inhibitors and were tested for their activity on HDAC isozymes and HDAC3. Compounds **T247** and **T326** (Scheme 22b) exhibited selective and potent HDAC3 inhibition. The anticancer activity on PC3 and HCT116 cells showed that the compound **T326** with a GI_{50} value of 0.94 μM on HCT116 and 1 μM was the most active.[87]

4β-(1,2,3-Triazol-1-yl)podophyllotoxin-based carbamates were synthesized (Scheme 23) and tested on HCT-8, HeLa, A-549, and HL-60 cells for anticancer activity. Few compounds were more active than the standard drug etoposide. Compound **16** (Figure 19) was most active with IC_{50} values of 0.01 μM to 0.51 μM against all the cell lines. The compounds acted by blocking the formation of microtubules by inhibiting DNA topoisomerase-II.[88]

Indoles linked via an alkyl-substituted triazole to *N*-hydroxyarylamides were synthesized (Scheme 24) and tested on MCF-7, HepG2, K562, HCT-116, and Lovo cells for their anticancer activity with SAHA as standard drug. Though most compounds produced good activity, compound **8n** (Figure 20) was most active with IC_{50} values (ranging from 3.57–6.21 μM), better than the standard drug SAHA for all the cell lines. The compounds were also tested for HDAC inhibitory activity. Compound **8n** produced excellent HDAC inhibition and was highly selective and potent toward HDAC1.[89]

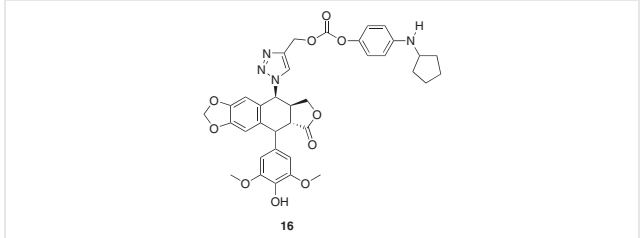

Figure 19 Structure of carbamate derivative **16**[88]

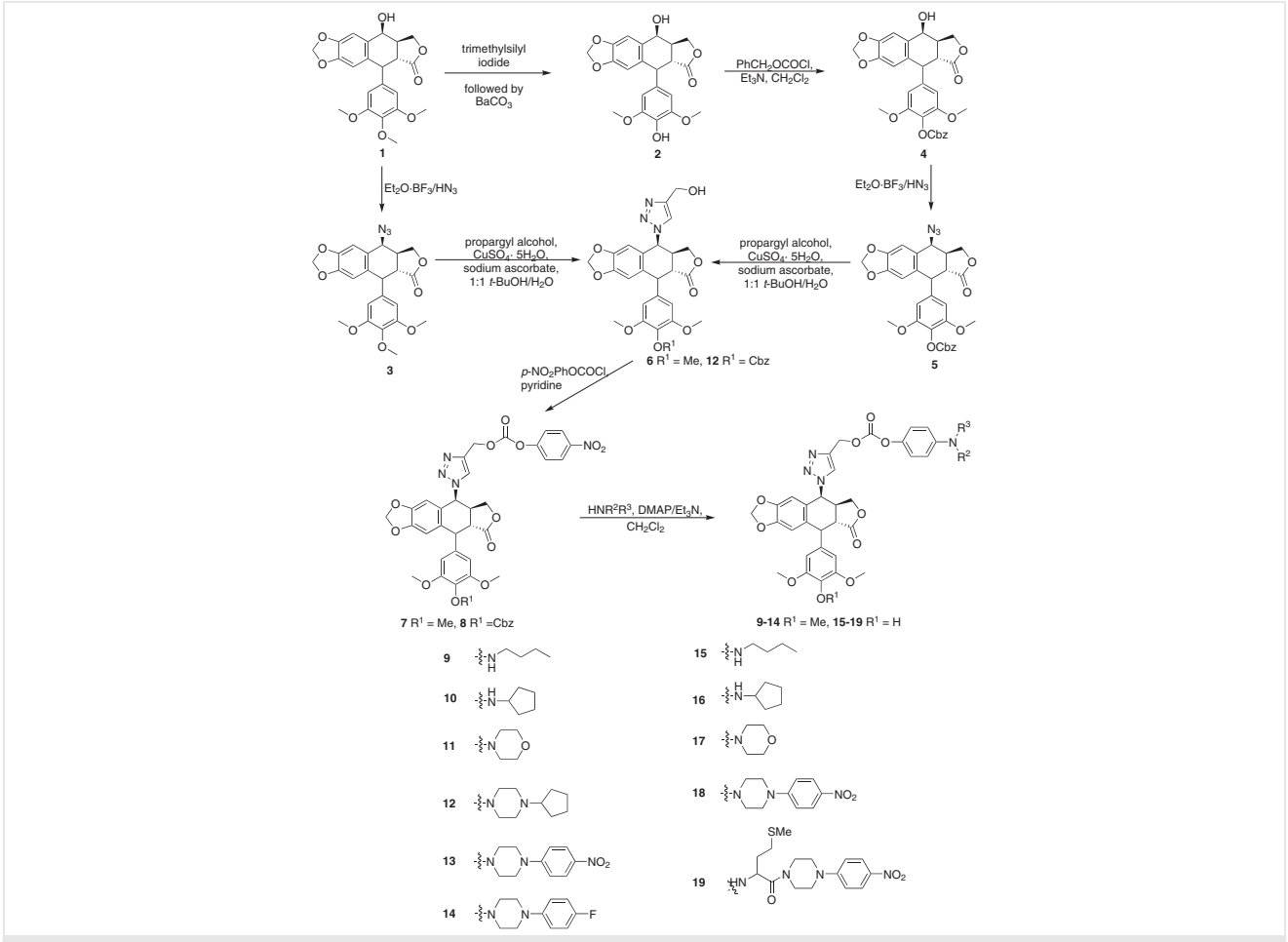

Scheme 23 Synthesis of carbamate derivatives of 4β-(1,2,3-triazol-1-yl)podophyllotoxin[88]

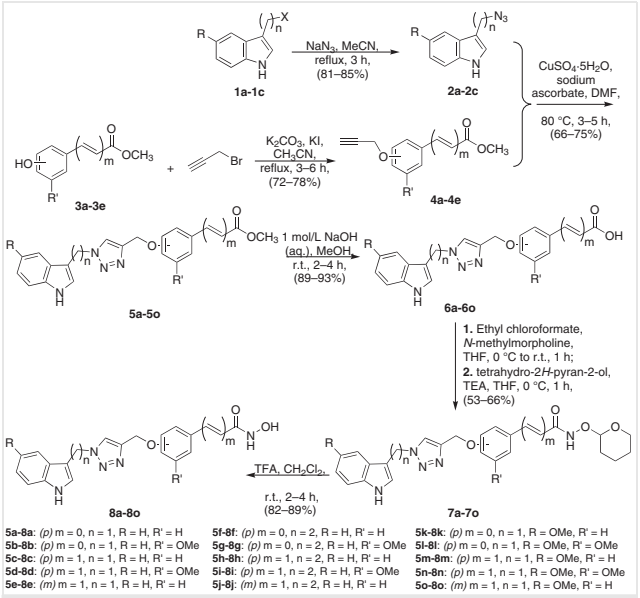

Scheme 24 Synthesis of indole-linked *N*-hydroxyarylamide derivatives[89]

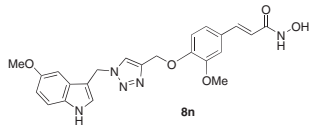

Figure 20 Structure of indole-linked *N*-hydroxyarylamide compound **8n**[89]

Taxoid, SB-T-1214 folate conjugate **13** (Scheme 25) was synthesized using copper-free click chemistry (Scheme 25) and the compound was then tested on WI-38(FR-), L1210-FR(FR^{++}), MX-1(FR^{++}), and ID8 (FR^{+++}) for their FR selective anticancer activity with paclitaxel as the standard drug. Compound **13** produced FR-specific cytotoxicity with IC_{50} values from 2.1–3.5 nM and was nontoxic toward normal cells at a dose of 5000 nM.[90]

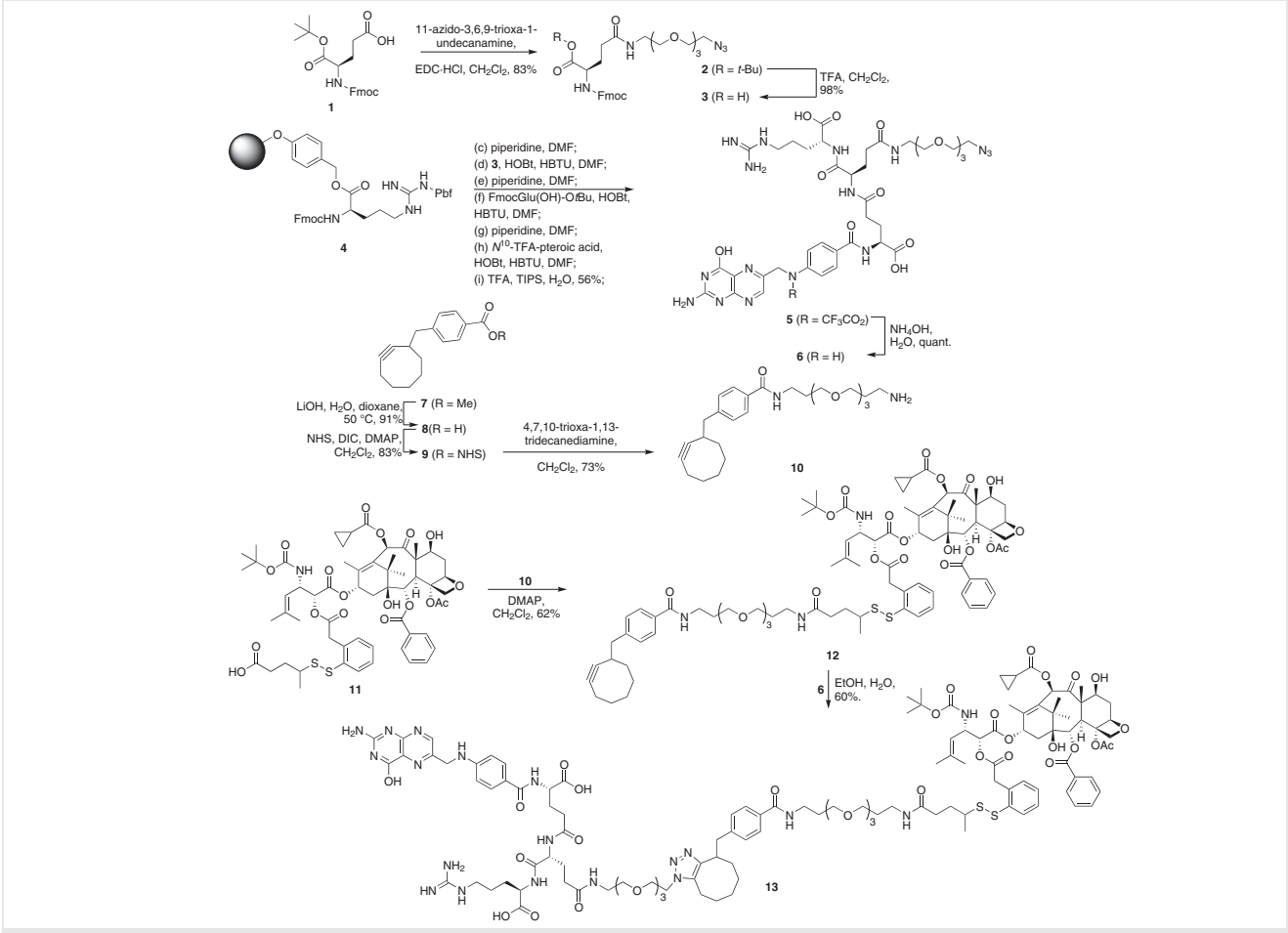

Scheme 25 Synthesis of folate–taxoid conjugate[90]

Coronopilin derivatives containing 1,2,3-triazoles were synthesized using click chemistry (Scheme 26) and were tested on MCF-7, A-549, HeLa, HCT-15, THP-1, and PC-3 cells for their anticancer activity. Most compounds produced good activity but compound **3a** (Figure 21), in particular, was the most active (IC_{50} ranging from 3.1–9.7 for all cell lines) among the synthesized compounds. The compound **3a** induced apoptosis in the G1 phase and was studied for NF-κB (p65) transcription factor inhibition and was found to produce 80% inhibition at 100 μM after 24 h. The type of connecting heteroatom between the triazole and the variable group determined the activity of 1,2,3-triazole-modified coronopilins. When the heteroatom was oxygen, the activity increased, and when it was nitrogen, it decreased. When halide-substituted phenyl rings were connected to the triazole ring via oxygen, the activity was at its peak.[91]

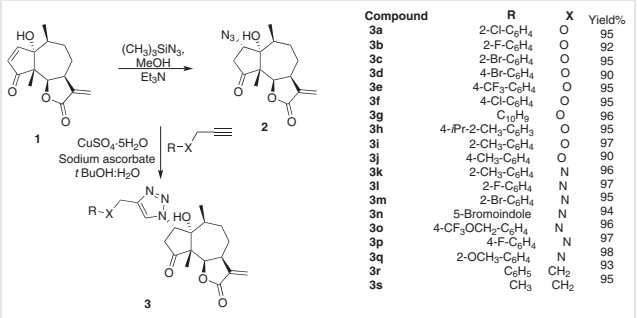

Compound	R	X	Yield%
3a	2-Cl-C_6H_4	O	95
3b	2-F-C_6H_4	O	92
3c	2-Br-C_6H_4	O	95
3d	4-Br-C_6H_4	O	90
3e	4-CF_3-C_6H_4	O	95
3f	4-Cl-C_6H_4	O	95
3g	$C_{10}H_9$	O	96
3h	4-*i*Pr-2-CH_3-C_6H_3	O	95
3i	2-CH_3-C_6H_4	O	97
3j	4-CH_3-C_6H_4	O	90
3k	2-CH_3-C_6H_4	N	96
3l	2-F-C_6H_4	N	97
3m	2-Br-C_6H_4	N	95
3n	5-Bromoindole	N	94
3o	4-CF_3OCH_2-C_6H_4	N	96
3p	4-F-C_6H_4	N	97
3q	2-OCH_3-C_6H_4	N	98
3r	C_6H_5	CH_2	93
3s	CH_3	CH_2	95

Scheme 26 Synthesis of coronopilin derivatives containing 1,2,3-triazoles[91]

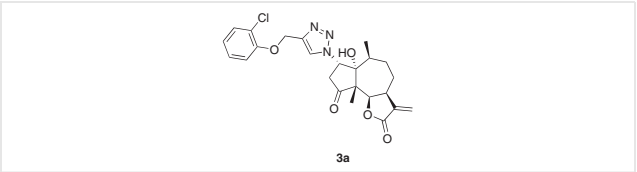

Figure 21 Structure of coronopilin derivative **3a**[91]

Synthesis of triazole- **15–26** and isoxazole-based 6-hydroxycoumarins **3–14** was performed using click chemistry (Scheme 27) and tested for anticancer activity on A-549, Colo-205, HCT-116, HL-60, and PC-3 cells. Though none of the compounds were as active as standard drug BEZ-235 except compound **10** on PC3 cells, some compounds were more active than 6-hydroxycoumarin. Isoxazole derivatives **10** and **13** (Figure 22) with IC_{50} values 8.2 and 13.6 μM, respectively, were most active on PC-3 cells and triazole derivatives **23** and **25** (Figure 22) with IC_{50} values 10.2 and 12.6 μM were most active on A-549 cells. Isoxazole derivatives with *ortho* substitution in the phenyl R group were effective cytotoxic agents against PC-3 cells, whilst triazoles with *ortho* substitution in the phenyl R′ were more effective against A-549 cells. It was also observed that nitro (NO_2) and cyano (CN) groups in the *ortho* position play an important role in achieving higher selectivity and activity.[92]

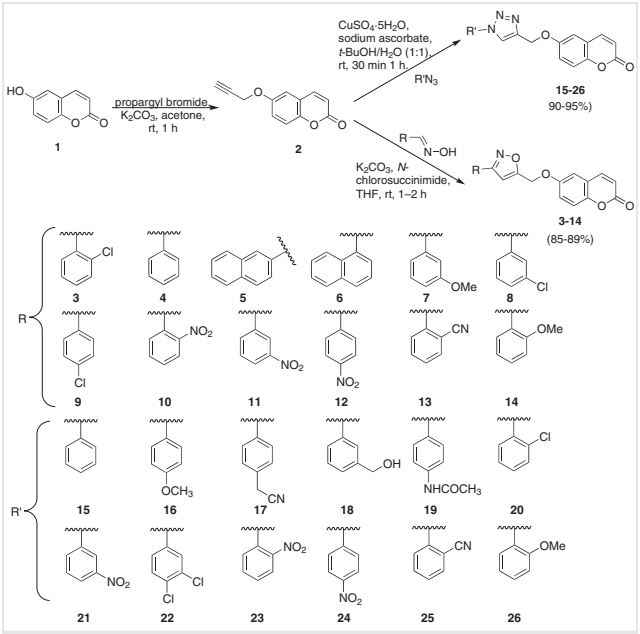

Scheme 27 Synthesis of triazole-and isoxazole-based 6-hydroxycoumarins[92]

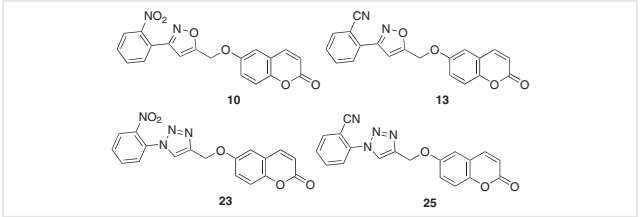

Figure 22 Structure of triazole- and isoxazole-based 6-hydroxycoumarins **10**, **13**, **23**, and **25**[92]

Cinchona alkaloids and monensin (MON) or salinomycin (SAL) conjugates were prepared using copper-catalyzed click chemistry (Scheme 28) and tested on HepG2, LoVo/Dx, and LoVo cells along with the normal cells (BALB/3T3) for their cytotoxic potential. None of the conjugates were as active as the parent compounds MON and SAL, but some of them produced less toxicity toward normal cells in comparison to doxorubicin and cisplatin.[93]

Triazole-based 4′-demethyl-epipodophyllotoxin and podophyllotoxin derivatives were synthesized using click chemistry (Scheme 29) and tested for their anticancer activity on A-549, COLO-205, PANC-1, and PC-3 cells. Some compounds produced better activity than the podophyllotoxin and compound **3k** (Figure 23) was most active (IC_{50} values 3.8–22 nM for all cell lines). The compound strongly stopped the motility of PC-3 cells.[94]

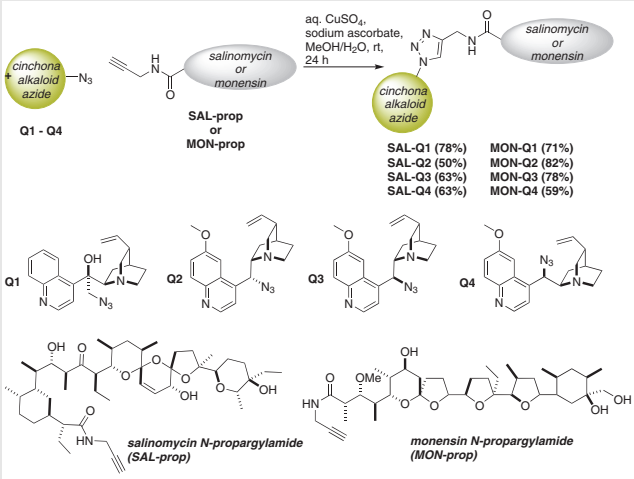

Scheme 28 Synthesis of cinchona alkaloids and monensin or salinomycin conjugates[93]

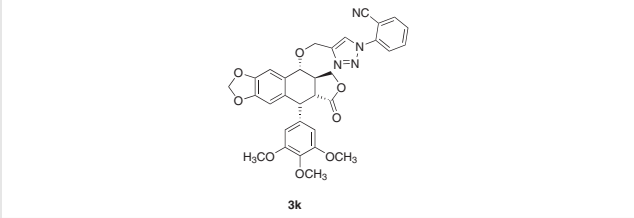

Figure 23 Structure of podophyllotoxin derivative **3k**[94]

4 Click Chemistry in Drug Delivery

Several chronic diseases, such as cancer, diabetes, and drug addiction, are treated and maybe cured in a significant way due to drug transportation. Yet, it might be challenging to meet the fundamental requirements and risk harming the way that medications work therapeutically because of their limited controllability and rapid release. Drugs are typically administered in strong doses at specific times. Lee and co-workers described the formation of hydrogels (TGs) containing triazoles that gradually expand when exposed to water. It was shown that hydrophobic aggregations, mostly brought on by stacking between triazole rings, are responsible for the time-dependent growth of the swelling (Figure 24). The hydrophobic region of this structure was gradually penetrated by water molecules, allowing a hydrogen bond to form between the water and one of the nitrogen atoms on the triazole ring.[18] This group has also described that the existence of ureido moieties, the chain length of the side groups, and the degree of quaternization (DQ) on the triazole ring were all key factors in the design of each polymer's upper critical solution temperature (UCST) in aqueous solution. To further regulate the UCSTs, methyl iodide quaternization processes were carried out on the triazole rings of each polymer. Findings demonstrated that the degree of quaternization might be used to accurately tailor the UCST.[17]

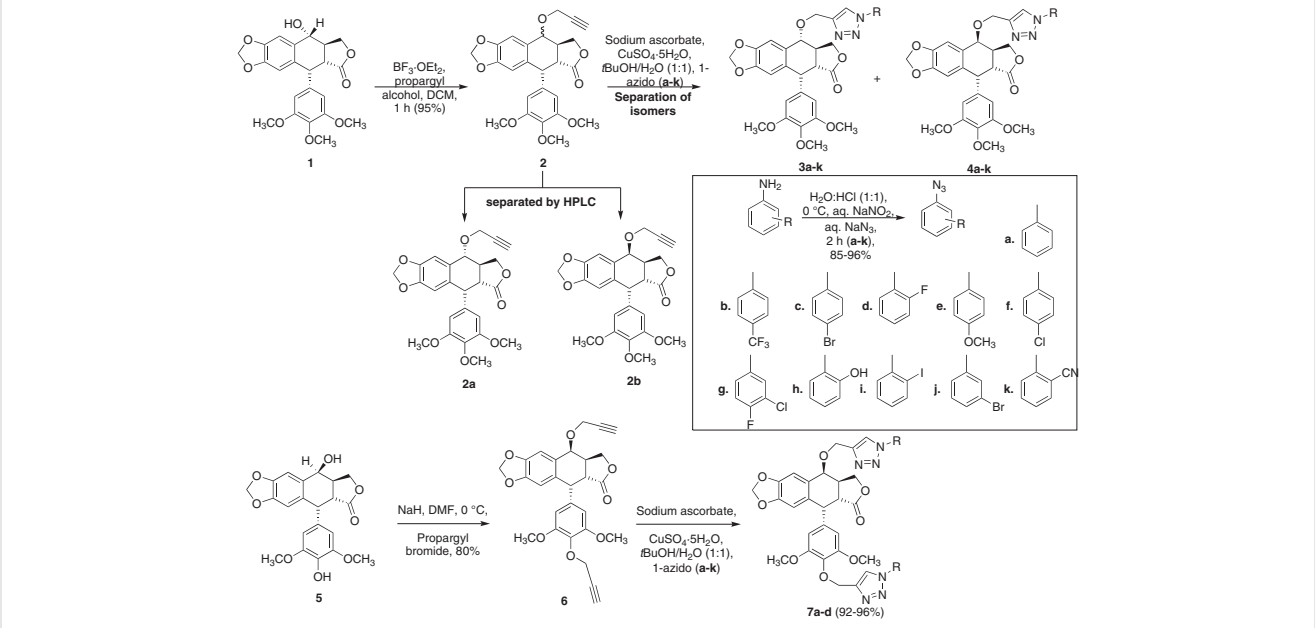

Scheme 29 Synthesis of triazole-based 4′-demethyl-epipodophyllotoxin and podophyllotoxin derivatives[94]

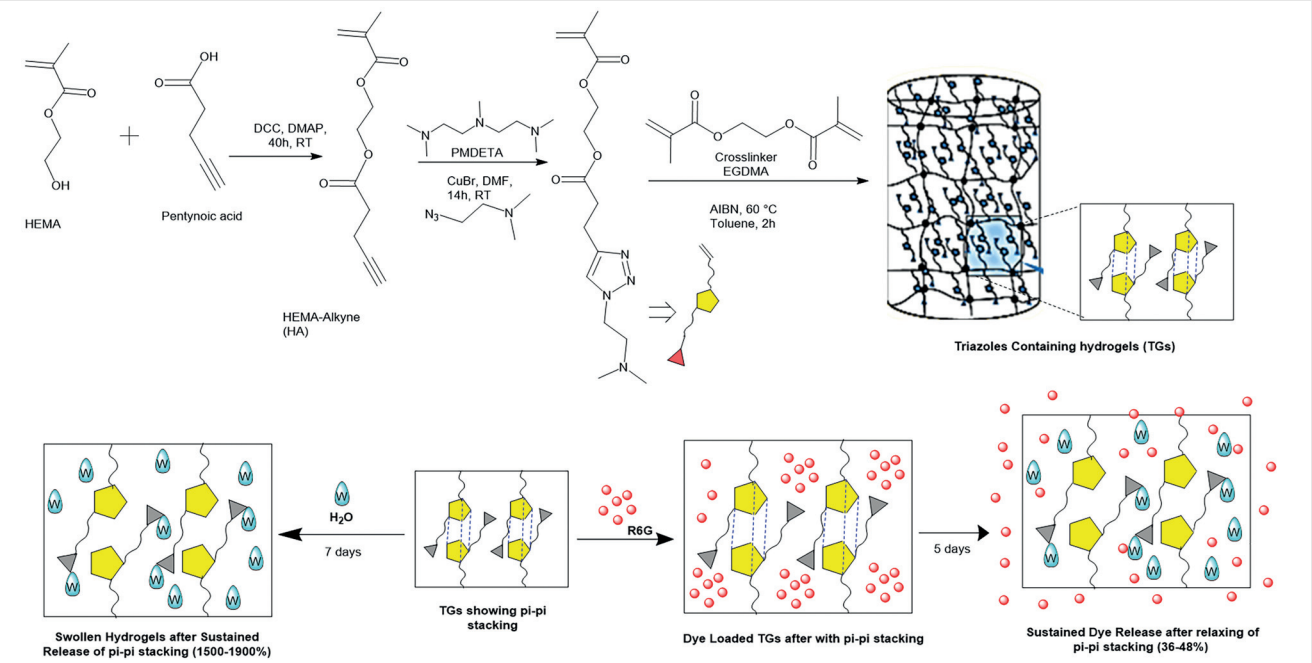

Figure 24 Triazole-containing hydrogels for time-dependent sustained drug release via stacking interaction between triazole rings[18]

Even though there are numerous effective nanocarriers for drug delivery, the US Food and Drug Administration (FDA) has only approved a small number of them for use in clinic therapy.[95,96] Because nanomedicines are difficult for cells to internalize in the majority of drug delivery systems, they have less of an impact on cancer cells.[97] Essentially, a micelle-based drug delivery system should easily pass through the cell membrane barriers of cancer cells and cause conjugated pharmaceuticals to leak inside the cells. According to a report, the electrostatic force easily causes positively charged micelles to adhere to the surfaces of negatively charged cell membranes, improving cellular internalization.[98]

Each targeted drug delivery system aims to create a framework for the nanodelivery formulations that will address the issues raised thus far by setting up a reagent-free click chemistry procedure. Currently, some observers believe that click chemistry is a meticulously planned strategy for creating novel molecular delivery systems. This innovative yet straightforward method relies mostly on the formation of carbon–heteroatom bonds using 'spring-loaded' reactants. The safety of the resulting carrier system is crucial to the success of the formulation. Additionally, particle sizes less than 300 nm serve to minimize opsonization of the proteins by macrophages in the body, which leads to premature removal of the formulation from the targeted tumor location. Hypoxia is a target that is prevalent in virtually all cancers and is usually located in the oxygen-deprived core of the tumor. Because of its position, it is difficult to target. However, the fast-growing cancer cells cause a shortage of oxygen and a drop in pH, resulting in the upregulation of the surface receptor CA IX. This is a useful cancer cell marker that helps the nanocarrier to penetrate to the core and so efficiently deliver the medicine to the targeted spot.

To overcome this, HAS-PTX (human serum albumin) carrying PTX (paclitaxel) was designed (Scheme 30) by Iyer, Sau, and co-workers for targeting CA IX (carbonic anhydrase) receptor for improving drug delivery to TNBC (triple negative breast cancer). ATZ (acetazolamide), a CA IX ligand, was used for the selective delivery of PTX. A new copper-free 'click' chemistry SPAAC (Strain-Promoted Alkyne Azide Cycloaddition) was used to combine azide and the DBCO (dibenzocyclooctyl) moiety. PTX was loaded using the desolvation method to form HSA-PTX-ATZ. The anticancer activity of the carriers was tested on MDA-MB-468 and MDA-MB-231. HSA-PTX-ATZ produced better anticancer activity than HSA-PTX, PTX, and HSA alone. Their findings of increased cell killing effects of HSA-PTX-ATZ in hypoxia compared to normoxia and higher absorption of rhodamine-labeled HSA-PTX-ATZ indicates that HSA-PTX-ATZ has a CA IX-mediated drug delivery impact.[99]

DOX (doxorubicin)-prodrug (pH-sensitive), 6MP(6–mercaptopurine)-prodrug were joined on to PDPAO [poly(DEA)-b-poly(ABMA-co-OEGMA), synthesized by RAFT (reversible addition-fragmentation chain transfer) polymerization[43,102,103]], by click chemistry (Scheme 31) to form PDPAO@imine-DOX/*cis*-6MP which further self-aggregated to polymeric M(DOX/6MP) micelles. These micelles produced pH-sensitive DOX release. These micelles cells showed enhanced cellular uptake and cytotoxic activity on

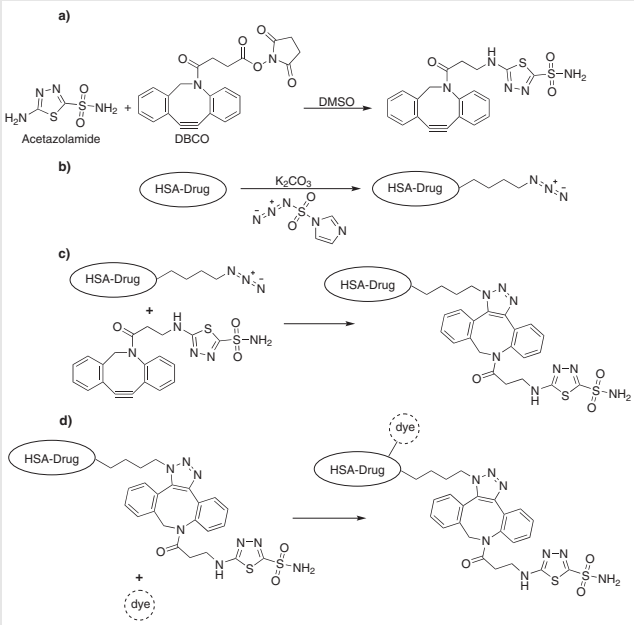

Scheme 30 Synthesis of HAS-PTX-ATZ[99]

HL-60 and HeLa cells. The cytotoxicity was adjustable with alterations in DOX and 6MP ratio. Higher cytotoxicity at 2:1 (DOX:6MP) was exhibited by the micelles. Because DOX and 6MP were conjugated to PDPAO via a 'click chemistry' process including an acid-labile imine bond and a Michael acceptor structure, endosomal/lysosomal pH-triggered DOX release and intracellular GSH-triggered 6MP release should be seen. Virtually all CI values against HL-60 cells were much lower than those against HeLa cells, showing that the combination techniques had a greater synergistic impact on HL-60 cells than on HeLa cells. This finding might be ascribed to intermolecular entanglement between DOX and 6MP, which slowed diffusion from the hydrophobic core area to the surface of micelles despite the fact that imine bond cleavage and Michael receptor addition were promoted in the intracellular microenvironment (pH 5.0 + GSH 10 mM). The current work proposes a synthesis technique for DOX and 6MP co-delivery on a polymeric platform that might enable both charge-conversion and successful combination treatment.[100]

PAMAM (polyamidoamine) based CTP (camptothecin) prodrug was synthesized (Scheme 32) using click chemistry. CTP was functionalized onto APO (1-azido-3,6,9,12,15-pentaoxaoctadecan-18-oic acid). Methoxypoly(ethylene glycol) amine and PPA (propargylamine) were conjugated to PAMAM dendrimer G4.5 using DMTMM (4-(4,6-dimethoxy-1,3,5-triazin-2-yl)-4-methylmorpholinium chloride). Finally, CTP-APO was coupled to the PEGylated PAMAM dendrimer (G4.5-PPA). The prodrug was tested for its anti-

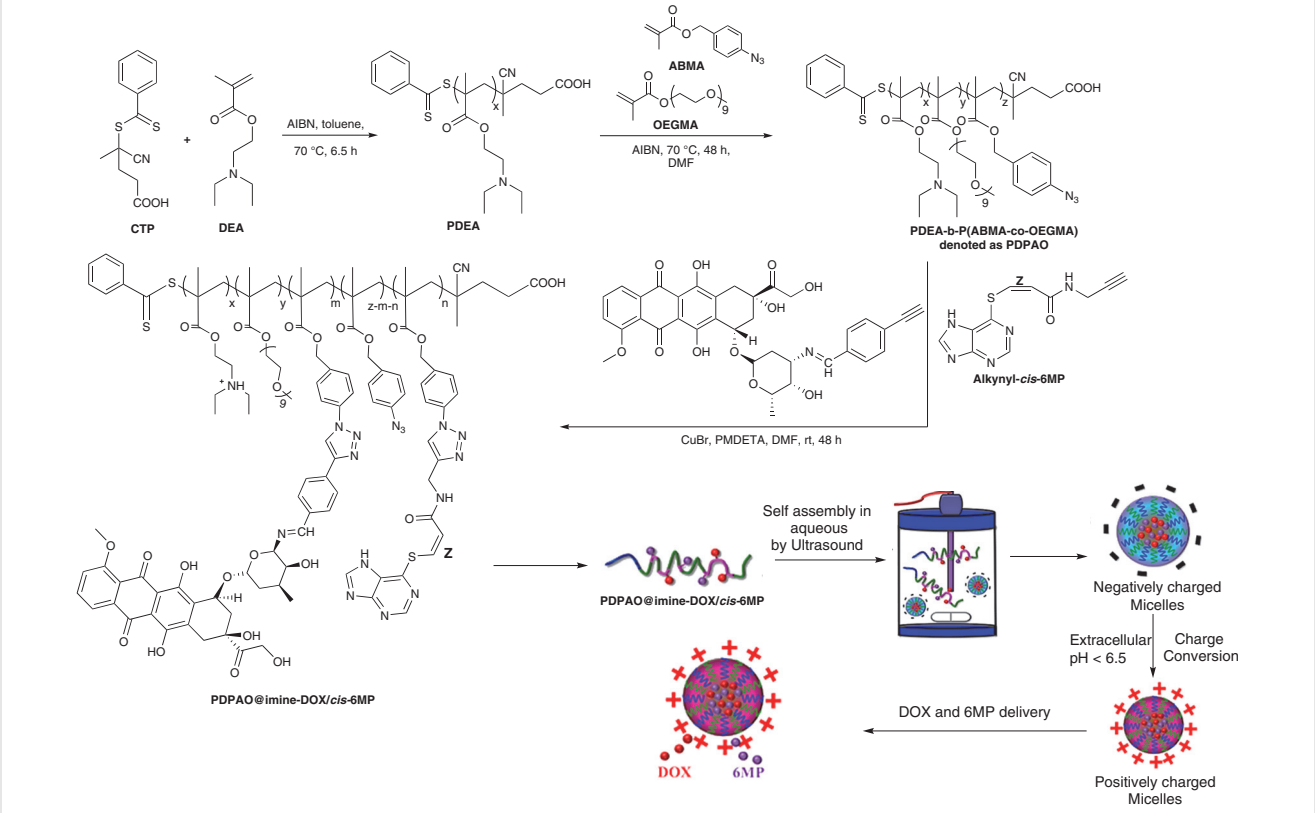

Scheme 31 Synthesis of PDPAO@imine-DOX/*cis*-6MP[100]

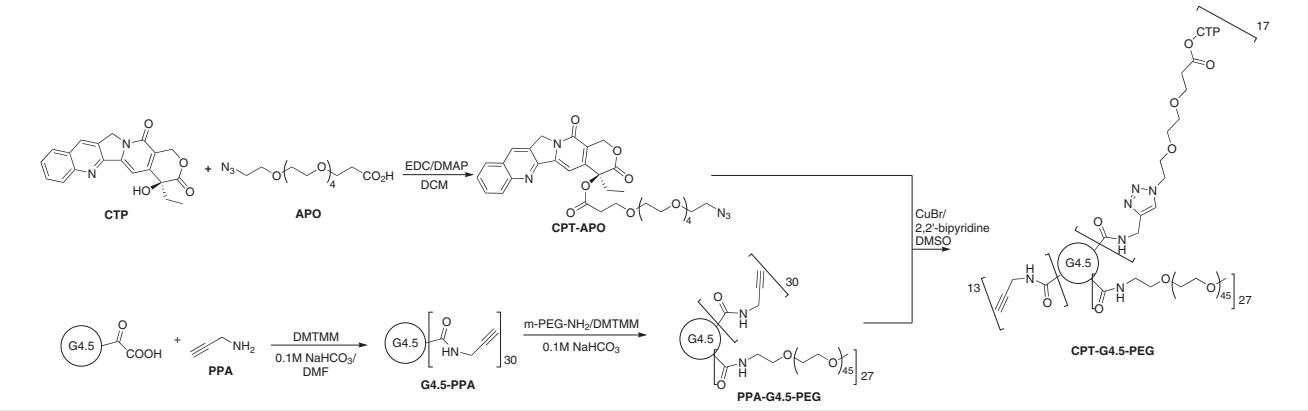

Scheme 32 Synthesis of PAMAM (polyamidoamine) based CTP (camptothecin) prodrug[101]

cancer potential on U1242 cell line and was found to have 185 times increase in activity (IC_{50} = 5 μM) relative to free CTP due to delayed release. The expanded usability of the click chemistry based coupling technique would allow for the production of large-scale high-quality polymer-drug-ligand conjugates with uniform ligand and drug loading on the dendrimer.[101]

5 Future Perspectives and Challenges

Click chemistry is a powerful tool for lead discovery and exploits combinatorial chemistry. As the triazole forming process is very reliable, fast, and leads to a near-perfect reaction it accelerates the process of lead optimization and lead finding.[104]

Copper-catalyzed reactions work well for alkyl or aryl azides, but electron-deficient azides do not respond well to this reaction. Also, the reactions only yield 1,4-disubstituted 1,2,3-triazoles and trisubstitution always remains challenging. Though there have been modified versions of this reaction to get 1,4,5-trisubstitution in triazoles. Copper-free methods have also been exploited but they have their challenges.[105–109]

6 Conclusion

Triazoles make up a variety of molecules and cover a wide spectrum of activity. In recent years triazole-based cycloadditions have been used in the development of new chemotherapeutic agents. Both copper-based and copper-free click chemistry reactions have been employed in the development of drug carriers like dendrimers and have also been used as a method to develop new anticancer molecules with some molecules producing excellent anticancer activities. The method has also been used to modify various natural products to develop better active compounds. Azide-alkyne click chemistry is still a reliable method to develop new molecules and could lead to the formation of a new molecule with excellent anticancer activity.

Conflict of Interest

The authors declare no conflict of interest.

Funding Information

V.M. is thankful to SERB New Delhi for TARE Project (TARE/2022/000673) for support.

Acknowledgment

Authors are thankful to Shoolini University, HP; Punjab University, Punjab, and Amity Institute of Click Chemistry Research and Studies, Amity University UP, India for all the support.

References

(1) Cancer: https://www.who.int/news-room/fact-sheets/detail/cancer (accessed Dec 13, 2022).
(2) Miller, K. D.; Siegel, R. L.; Lin, C. C.; Mariotto, A. B.; Kramer, J. L.; Rowland, J. H.; Stein, K. D.; Alteri, R.; Jemal, A. *Ca-Cancer J. Clin.* **2016**, *66*, 271.
(3) Caley, A.; Jones, R. *Surgery (Oxford)* **2012**, *30*, 186.
(4) Anand, P.; Kunnumakkara, A. B.; Newman, R. A.; Aggarwal, B. B. *Mol. Pharm.* **2007**, *4*, 807.
(5) Hu, C.-M. J.; Zhang, L. *Biochem. Pharmacol.* **2012**, *83*, 1104.
(6) Tang, Y.; Liang, J.; Wu, A.; Chen, Y.; Zhao, P.; Lin, T.; Zhang, M.; Xu, Q.; Wang, J.; Huang, Y. *ACS Appl. Mater. Interfaces* **2017**, *9*, 26648.
(7) Woodcock, J.; Griffin, J. P.; Behrman, R. E. *N. Engl. J. Med.* **2011**, *364*, 985.
(8) Peng, H.; Liu, X.; Wang, G.; Li, M.; Bratlie, K. M.; Cochran, E.; Wang, Q. *J. Mater. Chem. B* **2015**, *3*, 6856.
(9) Núñez, C.; Capelo, J. L.; Igrejas, G.; Alfonso, A.; Botana, L. M.; Lodeiro, C. *Biomaterials* **2016**, *97*, 34.

(10) Shim, G.; Kim, M.-G.; Kim, D.; Park, J. Y.; Oh, Y.-K. *Adv. Drug Delivery Rev.* **2017**, *115*, 57.
(11) Wu, L.; Leng, D.; Cun, D.; Foged, C.; Yang, M. *J. Controlled Release* **2017**, *260*, 78.
(12) Chaudhary, J.; Mavi, A. K.; Singh, N.; Srivastava, V. K.; Jyoti, A.; Kaushik, S.; Mishra, V. *Quaderns* **2023**, *11*, 294.
(13) Tsui, J. H.; Lee, W.; Pun, S. H.; Kim, J.; Kim, D.-H. *Adv. Drug Delivery Rev.* **2013**, *65*, 1575.
(14) Kolb, H. C.; Finn, M. G.; Sharpless, K. B. *Angew. Chem. Int. Ed.* **2001**, *40*, 2004.
(15) Dai, J.; Tian, S.; Yang, X.; Liu, Z. *Front. Chem.* **2022**, *10*, 891484; DOI: 10.3389/fchem.2022.891484.
(16) Tornøe, C. W.; Christensen, C.; Meldal, M. *J. Org. Chem.* **2002**, *67*, 3057.
(17) Mishra, V.; Jung, S.-H.; Jeong, H. M.; Lee, H. *Polym. Chem.* **2014**, *5*, 2411.
(18) Mishra, V.; Jung, S.-H.; Park, J. M.; Jeong, H. M.; Lee, H. *Macromol. Rapid Commun.* **2013**, *35*, 442.
(19) Golas, P. L.; Matyjaszewski, K. *QSAR Comb. Sci.* **2007**, *26*, 1116.
(20) Fournier, D.; Hoogenboom, R.; Schubert, U. S. *Chem. Soc. Rev.* **2007**, *36*, 1369.
(21) Nandivada, H.; Jiang, X.; Lahann, J. *Adv. Mater.* **2007**, *19*, 2197.
(22) Binder, W.; Kluger, C. *Curr. Org. Chem.* **2006**, *10*, 1791.
(23) Yadav, N.; Gaikwad, R. P.; Mishra, V.; Gawande, M. B. *Bull. Chem. Soc. Jpn.* **2022**, *95*, 1638.
(24) Yadav, N.; Mudgal, D.; Anand, R.; Jindal, S.; Mishra, V. *Int. J. Biol. Macromol.* **2022**, *220*, 537.
(25) Kolb, H. C.; Sharpless, K. B. *Drug Discovery Today* **2003**, *8*, 1128.
(26) Manetsch, R.; Krasiński, A.; Radić, Z.; Raushel, J.; Taylor, P.; Sharpless, K. B.; Kolb, H. C. *J. Am. Chem. Soc.* **2004**, *126*, 12809.
(27) Lenda, F.; Guenoun, F.; Tazi, B.; Ben Larbi, N.; Martinez, J.; Lamaty, F. *Tetrahedron Lett.* **2004**, *45*, 8905.
(28) Sivakumar, K.; Xie, F.; Cash, B. M.; Long, S.; Barnhill, H. N.; Wang, Q. *Org. Lett.* **2004**, *6*, 4603.
(29) Link, A. J.; Vink, M. K. S.; Tirrell, D. A. *J. Am. Chem. Soc.* **2004**, *126*, 10598.
(30) Meng, J.; Siuzdak, G.; Finn, M. G. *Chem. Commun.* **2004**, 2108.
(31) Wang, Q.; Chan, T. R.; Hilgraf, R.; Fokin, V. V.; Sharpless, K. B.; Finn, M. G. *J. Am. Chem. Soc.* **2003**, *125*, 3192.
(32) Gupta, S. S.; Mishra, V.; Mukherjee, M. D.; Saini, P.; Ranjan, K. R. *Int. J. Biol. Macromol.* **2021**, *188*, 542.
(33) Wu, Y.-M.; Deng, J.; Li, Y.; Chen, Q.-Y. *Synthesis* **2005**, 1314.
(34) Loren, J. C.; Sharpless, K. B. *Synthesis* **2005**, 1514.
(35) Bodine, K. D.; Gin, D. Y.; Gin, M. S. *J. Am. Chem. Soc.* **2004**, *126*, 1638.
(36) Suarez, P. L.; Gándara, Z.; Gómez, G.; Fall, Y. *Tetrahedron Lett.* **2004**, *45*, 4619.
(37) Li, Z.; Seo, T. S.; Ju, J. *Tetrahedron Lett.* **2004**, *45*, 3143.
(38) Kacprzak, K. *Synlett* **2005**, 943.
(39) Hou, J.; Liu, X.; Shen, J.; Zhao, G.; Wang, P. G. *Expert Opin. Drug Discovery* **2012**, *7*, 489.
(40) Kumar, M.; Verma, S.; Mishra, V.; Reiser, O.; Verma, A. K. *J. Org. Chem.* **2022**, *87*, 6263.
(41) Chatterjee, S.; Kumar, N.; Sehrawat, H.; Yadav, N.; Mishra, V. *Curr. Res. Green Sustainable Chem.* **2021**, *4*, 100064.
(42) Ngo, H. L.; Mishra, D. K.; Mishra, V.; Truong, C. C. *Chem. Eng. Sci.* **2021**, *229*, 116142.
(43) Mishra, V.; Kumar, R. *Polym. Sci., Ser. B* **2019**, *61*, 753.
(44) Kantheti, S.; Narayan, R.; Raju, K. V. S. N. *RSC Adv.* **2015**, *5*, 3687.
(45) Sahoo, S.; Sindhu, K. N.; Sreeveena, K. *Res. J. Pharm. Technol.* **2019**, *12*, 5091.
(46) Duran, A.; Dogan, H. N.; Rollas, S. *Farmaco* **2002**, *57*, 559.
(47) Manfredini, S.; Vicentini, C. B.; Manfrini, M.; Bianchi, N.; Rutigliano, C.; Mischiati, C.; Gambari, R. *Bioorg. Med. Chem.* **2000**, *8*, 2343.
(48) Johns, B. A.; Weatherhead, J. G.; Allen, S. H.; Thompson, J. B.; Garvey, E. P.; Foster, S. A.; Jeffrey, J. L.; Miller, W. H. *Bioorg. Med. Chem. Lett.* **2009**, *19*, 1802.
(49) Gujjar, R.; Marwaha, A.; El Mazouni, F.; White, J.; White, K. L.; Creason, S.; Shackleford, D. M.; Baldwin, J.; Charman, W. N.; Buckner, F. S.; Charman, S.; Rathod, P. K.; Phillips, M. A. *J. Med. Chem.* **2009**, *52*, 1864.
(50) Passannanti, A.; Diana, P.; Barraja, P.; Mingoia, F.; Lauria, A.; Cirrincione, G. *Heterocycles* **1998**, *48*, 1229.
(51) Guan, L.; Jin, Q.; Tian, G.; Chai, K.; Quan, Z. *J. Pharm. Pharm. Sci.* **2007**, *10*, 254.
(52) Banu, K.; Dinakar, A.; Ananthanarayanan, C. *Indian J. Pharm. Sci.* **1999**, *61*, 202.
(53) Hafez, H.; Abbas, H.-A.; El-Gazzar, A.-R. *Acta Pharm.* **2008**, *58*, 359.
(54) Sheremet, E. A.; Tomanov, R. I.; Trukhin, E. V.; Berestovitskaya, V. M. *Russ. J. Org. Chem.* **2004**, *40*, 594.
(55) Chen, M.; Lu, S.; Yuan, G.; Yang, S.; Du, X. *Heterocycl. Commun.* **2000**, *6*, 421.
(56) Kharb, R.; Sharma, P. C.; Yar, M. S. *J. Enzyme Inhib. Med. Chem.* **2011**, *26*, 1.
(57) Chatterjee, S.; Mishra, V. *Curr. Res. Green Sustainable Chem.* **2020**, *3*, 100025.
(58) Srivastava, A.; Mishra, V.; Singh, P.; Kumar, R. *J. Appl. Polym. Sci.* **2012**, *126*, 395.
(59) Mohammed, I.; Kummetha, I. R.; Singh, G.; Sharova, N.; Lichinchi, G.; Dang, J.; Stevenson, M.; Rana, T. M. *J. Med. Chem.* **2016**, *59*, 7677.
(60) Bonandi, E.; Christodoulou, M. S.; Fumagalli, G.; Perdicchia, D.; Rastelli, G.; Passarella, D. *Drug Discovery Today* **2017**, *22*, 1572.
(61) Horne, W. S.; Yadav, M. K.; Stout, C. D.; Ghadiri, M. R. *J. Am. Chem. Soc.* **2004**, *126*, 15366.
(62) Dondoni, A.; Marra, A. *J. Org. Chem.* **2006**, *71*, 7546.
(63) Hotha, S.; Kashyap, S. *J. Org. Chem.* **2006**, *71*, 364.
(64) *Design of Hybrid Molecules for Drug Development*; Decker, M., Ed.; Elsevier: Amsterdam, **2017**.
(65) Himo, F.; Lovell, T.; Hilgraf, R.; Rostovtsev, V. V.; Noodleman, L.; Sharpless, K. B.; Fokin, V. V. *J. Am. Chem. Soc.* **2005**, *127*, 210.
(66) Gholampour, M.; Ranjbar, S.; Edraki, N.; Mohabbati, M.; Firuzi, O.; Khoshneviszadeh, M. *Bioorg. Chem.* **2019**, *88*, 102967.
(67) Ding, Y.; Guo, H.; Ge, W.; Chen, X.; Li, S.; Wang, M.; Chen, Y.; Zhang, Q. *Eur. J. Med. Chem.* **2018**, *156*, 216.
(68) Hou, W.; Luo, Z.; Zhang, G.; Cao, D.; Li, D.; Ruan, H.; Ruan, B. H.; Su, L.; Xu, H. *Eur. J. Med. Chem.* **2017**, *138*, 1042.
(69) Khattab, R. R.; Alshamari, A. K.; Hassan, A. A.; Elganzory, H. H.; El-Sayed, W. A.; Awad, H. M.; Nossier, E. S.; Hassan, N. A. *J. Enzyme Inhib. Med. Chem.* **2021**, *36*, 504.
(70) Nguyen, B. C. Q.; Takahashi, H.; Uto, Y.; Shahinozzaman, M.; Tawata, S.; Maruta, H. *Eur. J. Med. Chem.* **2017**, *126*, 270.
(71) Jordan, B. C.; Kumar, B.; Thilagavathi, R.; Yadhav, A.; Kumar, P.; Selvam, C. *Chem. Biol. Drug Des.* **2018**, *91*, 332.
(72) Chavan, P. V.; Desai, U. V.; Wadgaonkar, P. P.; Tapase, S. R.; Kodam, K. M.; Choudhari, A.; Sarkar, D. *Bioorg. Chem.* **2019**, *85*, 475.
(73) Vishnuvardhan, M. V. P. S.; Saidi Reddy, V.; Chandrasekhar, K.; Lakshma Nayak, V.; Bin Sayeed, I.; Alarifi, A.; Kamal, A. *MedChemComm* **2017**, *8*, 1817.
(74) Li, X.; Wu, Y.; Wang, Y.; You, Q.; Zhang, X. *Molecules* **2017**, *22*, 1834.

(75) Hadiyal, S. D.; Lalpara, J. N.; Parmar, N. D.; Joshi, H. S. *Polycyclic Aromat. Compd.* **2022**, *42*, 4752.
(76) Shakeel-u-Rehman, ; Bhat, K. A.; Lone, S. H.; Malik, F. A. *Arabian J. Chem.* **2019**, *12*, 3479.
(77) Sahay, I. I.; Ghalsasi, P. S. *Synth. Commun.* **2017**, *47*, 825.
(78) Djemoui, A.; Naouri, A.; Ouahrani, M. R.; Djemoui, D.; Lahcene, S.; Lahrech, M. B.; Boukenna, L.; Albuquerque, H. M. T.; Saher, L.; Rocha, D. H. A.; Monteiro, F. L.; Helguero, L. A.; Bachari, K.; Talhi, O.; Silva, A. M. S. *J. Mol. Struct.* **2020**, *1204*, 127487.
(79) Naouri, A.; Djemoui, A.; Ouahrani, M. R.; Lahrech, M. B.; Lemouari, N.; Rocha, D. H. A.; Albuquerque, H.; Mendes, R. F.; Almeida Paz, F. A.; Helguero, L. A.; Bachari, K.; Talhi, O.; Silva, A. M. S. *J. Mol. Struct.* **2020**, *1217*, 128325.
(80) Lone, S. H.; Bhat, K. A.; Majeed, R.; Hamid, A.; Khuroo, M. A. *Bioorg. Med. Chem. Lett.* **2014**, *24*, 1047.
(81) Nagesh, H. N.; Suresh, N.; Prakash, G. V. S. B.; Gupta, S.; Rao, J. V.; Sekhar, K. V. G. C. *Med. Chem. Res.* **2015**, *24*, 523.
(82) Farooq, S.; Shakeel-u-Rehman, ; Hussain, A.; Hamid, A.; Qurishi, M. A.; Koul, S. *Eur. J. Med. Chem.* **2014**, *84*, 545.
(83) Tian, Y.; Liang, Z.; Xu, H.; Mou, Y.; Guo, C. *Molecules* **2016**, *21*, 758.
(84) Singh, J.; Sharma, S.; Saxena, A. K.; Nepali, K.; Bedi, P. M. S. *Med. Chem. Res.* **2013**, *22*, 3160.
(85) Huang, Z.-H.; Zhuo, S.-T.; Li, C.-Y.; Xie, H.-T.; Li, D.; Tan, J.-H.; Ou, T.-M.; Huang, Z.-S.; Gu, L.-Q.; Huang, S.-L. *Eur. J. Med. Chem.* **2013**, *68*, 58.
(86) Khaybullin, R.; Zhang, M.; Fu, J.; Liang, X.; Li, T.; Katritzky, A. R.; Okunieff, P.; Qi, X. *Molecules* **2014**, *19*, 18676.
(87) Suzuki, T.; Kasuya, Y.; Itoh, Y.; Ota, Y.; Zhan, P.; Asamitsu, K.; Nakagawa, H.; Okamoto, T.; Miyata, N. *PLoS One* **2013**, *8*, e68669.
(88) Liu, J.-F.; Sang, C.-Y.; Xu, X.-H.; Zhang, L.-L.; Yang, X.; Hui, L.; Zhang, J.-B.; Chen, S.-W. *Eur. J. Med. Chem.* **2013**, *64*, 621.
(89) Cai, M.; Hu, J.; Tian, J.-L.; Yan, H.; Zheng, C.-G.; Hu, W.-L. *Chin. Chem. Lett.* **2015**, *26*, 675.
(90) Seitz, J. D.; Vineberg, J. G.; Herlihy, E.; Park, B.; Melief, E.; Ojima, I. *Bioorg. Med. Chem.* **2015**, *23*, 2187.
(91) Khazir, J.; Hyder, I.; Gayatri, J. L.; Prasad Yandrati, L.; Nalla, N.; Chasoo, G.; Mahajan, A.; Saxena, A. K.; Alam, M. S.; Qazi, G. N.; Sampath Kumar, H. M. *Eur. J. Med. Chem.* **2014**, *82*, 255.
(92) Shakeel-u-Rehman, ; Masood-ur-Rahman, ; Tripathi, V. K.; Singh, J.; Ara, T.; Koul, S.; Farooq, S.; Kaul, A. *Bioorg. Med. Chem. Lett.* **2014**, *24*, 4243.
(93) Skiera, I.; Antoszczak, M.; Trynda, J.; Wietrzyk, J.; Boratyński, P.; Kacprzak, K.; Huczyński, A. *Chem. Biol. Drug Des.* **2015**, *86*, 911.
(94) Zilla, M. K.; Nayak, D.; Vishwakarma, R. A.; Sharma, P. R.; Goswami, A.; Ali, A. *Eur. J. Med. Chem.* **2014**, *77*, 47.
(95) Ganivada, M. N.; Rao, N. V.; Dinda, H.; Kumar, P.; Sarma, J. D.; Shunmugam, R. *Macromolecules* **2014**, *47*, 2703.
(96) Wang, Q.; Cheng, H.; Peng, H.; Zhou, H.; Li, P. Y.; Langer, R. *Adv. Drug Delivery Rev.* **2015**, *91*, 125.
(97) Mao, J.; Li, Y.; Wu, T.; Yuan, C.; Zeng, B.; Xu, Y.; Dai, L. *ACS Appl. Mater. Interfaces* **2016**, *8*, 17109.
(98) Yuan, Y.-Y.; Mao, C.-Q.; Du, X.-J.; Du, J.-Z.; Wang, F.; Wang, J. *Adv. Mater.* **2012**, *24*, 5476.
(99) Tatiparti, K.; Sau, S.; Gawde, K. A.; Iyer, A. K. *Int. J. Mol. Sci.* **2018**, *19*, 838.
(100) Liao, J.; Peng, H.; Wei, X.; Song, Y.; Liu, C.; Li, D.; Yin, Y.; Xiong, X.; Zheng, H.; Wang, Q. *Mater. Sci. Eng.: C* **2020**, *108*, 110461.
(101) Zolotarskaya, O. Y.; Xu, L.; Valerie, K.; Yang, H. *RSC Adv.* **2015**, *5*, 58600.
(102) Mishra, V.; Kumar, R. *J. Sci. Res. Banaras Hindu Univ.* **2012**, *56*, 141.
(103) Mishra, V.; Kumar, R. *J. Appl. Polym. Sci.* **2011**, *124*, 4475.
(104) Agalave, S. G.; Maujan, S. R.; Pore, V. S. *Chem. Asian J.* **2011**, *6*, 2696.
(105) Jiang, X.; Hao, X.; Jing, L.; Wu, G.; Kang, D.; Liu, X.; Zhan, P. *Expert Opin. Drug Discovery* **2019**, *14*, 779.
(106) Spiteri, C.; Moses, J. E. *Angew. Chem. Int. Ed.* **2010**, *49*, 31.
(107) Tiwari, V. K.; Mishra, B. B.; Mishra, K. B.; Mishra, N.; Singh, A. S.; Chen, X. *Chem. Rev.* **2016**, *116*, 3086.
(108) Lee, H.; Lee, J. K.; Min, S.-J.; Seo, H.; Lee, Y.; Rhee, H. *J. Org. Chem.* **2018**, *83*, 4805.
(109) Pereira, D.; Pinto, M.; Correia-da-Silva, M.; Cidade, H. *Molecules* **2022**, *27*, 230.